Available online at www.synsint.com

Synthesis and Sintering

ISSN 2564-0186 (Print), **ISSN** 2564-0194 (Online)

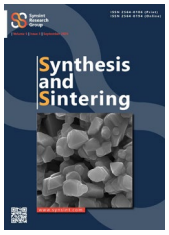

Review article

A review of enhanced hydrogen storage in MgH_2: the role of high-energy reactive ball milling and catalysis

Ali Borchloo [a,*], **Khanali Nekouee** [b]

[a] *Center for Nanoscience and Nanotechnology, Institute for Convergence Science & Technology, Sharif University of Technology, Tehran 14588-89694, Iran*

[b] *Faculty of Materials and Manufacturing Technologies, Malek Ashtar University of Technology, Tehran, Iran*

ABSTRACT

Due to its significant hydrogen capacity (7.6 wt%), availability, and reversibility, magnesium hydride (MgH_2) is considered one of the most promising solid-state hydrogen storage materials, making it attractive for sustainable energy systems. The excellent thermodynamic stability and slow absorption/desorption kinetics, which require elevated operating temperatures, limit its practical application. This paper addresses the important issue of how advanced synthesis methods, specifically high-energy reactive ball milling and catalytic doping, can overcome inherent challenges and enable the practical use of MgH_2 for hydrogen storage. The methodology adopted is a systematic and integrative review of state-of-the-art experimental and theoretical studies, focusing on thermodynamic and kinetic fundamentals, synthesis routes, catalytic additives, and nanostructuring strategies. Results indicate that high-energy ball milling significantly improves hydrogen diffusion by reducing particle sizes to the nanoscale and lowering the desorption onset temperature by approximately 45 °C. Catalysts such as 2 mol% Nb_2O_5 further reduce activation energy barriers, enabling rapid hydrogen release of 6.4 wt% in 114 s, while polymorphic transitions (γ-MgH_2 formation) enhance structural stability. Despite these advances, challenges such as grain coarsening and cycling capacity loss remain, highlighting the importance of nanoencapsulation, alloying, and scalable fabrication techniques. In conclusion, the review provides a critical framework for understanding the synergistic role of ball milling and catalysis in tailoring MgH_2 properties and outlines future research directions toward efficient, scalable, and application-ready hydrogen storage systems.

KEYWORDS

MgH_2
Hydrogen storage
Thermodynamics
High-energy reactive ball milling
Catalysis

OPEN ACCESS

1. Introduction

Crude oil, natural gas, coal, and other fossil fuels account for almost 85% of global energy production. This monopoly has resulted in high carbon dioxide emissions, global warming, environmental hazards from drilling, and unstable sources. The transition to renewable energy sources is a substantial challenge. Hydrogen, a promising renewable energy carrier, works well with intermittent renewable energy systems, allowing surplus energy to be stored and used during peak hours. This option is highly favorable for sustainable energy carriers because of its impressive energy density and the fact that its combustion results solely in water production. However, the basic issue is safe and effective storage, which is a major impediment to widespread adoption [1].

Magnesium hydride, a possible material for solid-state hydrogen storage, is lightweight, inexpensive, and abundant, with a hydrogen density. It accounts for 2.76% of the Earth's crust and 0.14% of

* Corresponding author. *E-mail address:* ali.borchloo77@sharif.edu (A. Borchloo)

Received 16 July 2025; Received in revised form 19 September 2025; Accepted 20 September 2025.

https://doi.org/10.53063/synsint.2025.53296

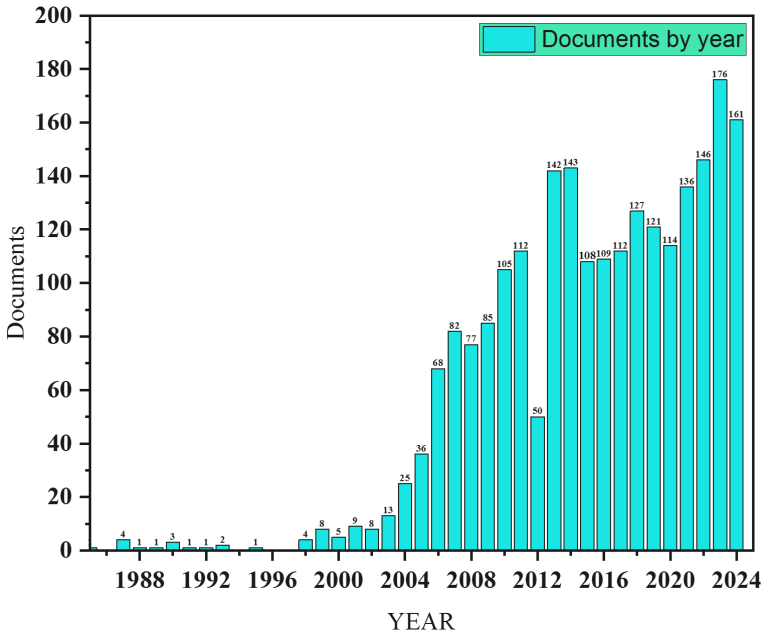

Fig. 1. Literature search results of different years in Scopus on hydrogen storage based on magnesium hydride (MgH_2) as keywords and data received from Scopus.

saltwater. However, the sluggish adsorption and desorption kinetics of hydrogen, as well as the high operating temperatures, limit its applicability [2]. Fig. 1 shows the rapid increase in Scopus publications on magnesium hydride and hydrogen storage. It is known that since 2000, the production of hydrogen storage based on magnesium hydride has greatly increased. Thermodynamic laws dictate that H_2 absorption from MgH_2 occurs at relatively high temperatures, T (1 bar) = 283 °C. In addition to this, the effective calculations of the enthalpy and entropy change of bulk MgH_2 are as follows: ΔH_{dec}=74.06±0.42 kJ/mol and ΔS=133.4±0.7 J/(mol.K) [2, 3]. The creation of a workable hydrogen storage material has nevertheless advanced significantly, and this paper reviews recent advancements over the last five years, especially as they relate to hydrogen-based energy storage.

In general, the adsorption and desorption of H_2 from magnesium hydride are affected by temperature, which is very important for its practical application in hydrogen storage. Absorption temperature is the process by which hydrogen gas is absorbed by magnesium to form magnesium hydride, which occurs at temperatures between 300 and 400 °C. During this process, hydrogen molecules first contact the surface of magnesium (Mg) particles, and then hydrogen molecules are decomposed after interacting with the magnesium surface. Then, hydrogen atoms penetrate the magnesium lattice and grow to form magnesium hydride (MgH_2) [4, 5]. Its general chemical reaction includes:

$$Mg + H_2 \rightarrow MgH_2 \quad (1)$$

Desorption is also a process in which hydrogen is released from magnesium hydride, which involves breaking the chemical bonds between magnesium and hydrogen and releasing hydrogen gas, which has a temperature of about 283 °C. Heating breaks the magnesium-hydrogen bonds in MgH_2. This phase is endothermic, and when hydrogen atoms are released from their bonds with magnesium, they diffuse through the MgH_2 matrix on the surface. Also, the diffusion process is influenced by the microstructure of the material [6]. The nanostructure and presence of defects can facilitate faster diffusion pathways.

$$MgH_2 \rightarrow Mg + H_2 \quad (2)$$

Moreover, the kinetics of desorption are influenced by both temperature and pressure. Higher temperatures provide increased thermal energy, which generally speeds up the desorption process. Lower hydrogen pressures and nano-scale materials increase the rate of absorption. The use of catalysts and additives, such as transition metals, can reduce the activation energy required for the desorption process, thereby releasing hydrogen at lower temperatures [6, 7].

High temperatures accelerate hydrogen absorption by supplying energy for hydrogen separation and release [8]. Adding catalysts such as transition metals increases adsorption kinetics, whereas encapsulating MgH_2 nanostructures improves hydrogen release and absorption kinetics [9]. Mechano-synthesized nanostructures produce flaws, boosting the kinetic rates of hydrogen diffusion. Additives such as transition metals and oxides can also boost reaction kinetics [7]. Magnesium forms the dihydride stoichiometry as MgH_2, which crystallizes into two polymorphic structures. Stability in such environmental conditions makes α-MgH_2 possess a tetragonal rutile TiO_2 structure. This hydride, at high applied pressures of more than 0.39 GPa (3.9 kbar) [10], undergoes an unstable change, under normal conditions, into γ-MgH_2, which crystallizes with a α-PbO_2 type structure [8].

The hexagonal closed magnesium lattice (HCP) grows by around 30% after hydrogenation (31.4% for α-MgH_2 and 29.1% for γ-MgH_2) (Table 1). The HCP metallic sublattice undergoes hydrogenation and becomes a deformed, body-centered cubic sublattice. This sublattice becomes orthogonal for γ-MgH_2. Even if the α-γ transformation is accompanied by a volume contraction of 1.3%, the main structural features of the dihydrides remain the same for both hydrides [11].

Table 1. Changing transitions in the metallic sublattice during the Mg-MgH_2 transition [8].

Hydride	H/Mg (at%)	Metal structure	V_m (Å^3)	Hydride structure	V_h (Å^3)	$\frac{V_h - V_m}{V_m}$ (%)	Ref.
α-MgH_2	2	HCP	23.2	TiO_2	30.53	31.4	[12]
γ-MgH_2	2	HCP	23.2	α-PbO_2	30.01	29.1	[13]

Magnesium and aluminum often exhibit comparable behaviors. In both cases, a small quantity of metal atoms, two in the AlH_3 structure and three in the MgH_2 structure, connect the gaps instead of occupying them with H atoms. The evidence of the covalent connection between them is clearly demonstrated by this discovery. In the α-MgH_2 structure, MgH_6 octahedra interconnect through their edges, forming chains.

The advancement of safe, effective, and affordable hydrogen storage solutions is crucial for reducing carbon emissions, enhancing the efficiency of clean renewable energy consumption, and harnessing hydrogen energy. Technologies for compressed gaseous hydrogen storage have maintained a prominent role in this sector due to their advantages in efficiency, low energy consumption, user-friendliness, and simplicity [14]. Solid-state hydrogen storage technologies, which are regarded as a promising hydrogen storage method, use metal hydrides in their industrial applications. The metal hydride-based hydrogen storage method can effectively overcome the shortcomings of other hydrogen storage techniques due to its high volumetric hydrogen storage density, ease of use, portability, affordability, and high device safety, as well as the ability to choose the right fuel for the vehicle [15–17].

Alloying is generally a straightforward and established technique for changing Mg/MgH_2. The thermodynamic characteristics of MgH_2 can be successfully enhanced by introducing alloying elements to the Mg/MgH_2 system to alter the water reaction routes and hydrogen absorption. Reilly et al. [18] first discovered that the Mg_2Ni intermetallic compound, which is produced by adding the alloying element Ni to the Mg/MgH_2 system, had good thermodynamic performance for hydrogen adsorption and desorption. In order to exert the hydrogen storage capabilities of their respective alloying compounds, Fe, Co, Si, Cu, and other alloying elements are then added to the Mg/MgH_2 system. Nevertheless, the main drawback of alloying is that capacity is lost when all alloying elements are used, and certain magnesium-based hydrogen storage alloys exhibit an irreversible hydrogen absorption or desorption process [19].

As a result, employing catalysts to improve the kinetics of MgH_2 hydrogen storage has been a common and successful strategy since the 1990s. These catalysts include carbides, halides, transition metals, and transition metal oxides. In addition to the catalyst, the development of hydrogen storage composites through the combination of complex hydrides with MgH_2 has been a popular research topic in recent years [20]. Also, Table 2 lists the names and short forms referenced in this overview are provided in.

Also, studies in recent years have shown that the nanoscale of magnesium hydride, due to the accumulation and inevitable growth of additives, has led to the improvement of MgH_2 hydrogen storage performance in recent years [6, 21, 22]. The particle size of MgH_2 generally affects its kinetics and thermodynamics by changing the surface-to-volume ratio. Since smaller particles usually have a higher surface-to-volume ratio than larger particles, they can supply the reactivity and reaction rate of MgH_2. In keeping with smaller crystal sizes, they also have more surface area, more nucleation sites, and a shorter path for the absorption and desorption of hydrogen. The size of the MgH_2 crystal in that material can affect the nucleation and formation of new phases, the overall crystal structure of the material, and ultimately the reaction kinetics and thermodynamics [4]. Additionally, schematic representations of basic theories and approaches for magnesium-based hydrogen storage material nanostructures are shown in Fig. 2.

Table 2. Nomenclatures are mentioned in this review.

Nomenclature	Description	Unit
Mg	Magnesium	–
H_2	Hydrogen molecule	–
MgH_2	Magnesium hydride	–
γ-MgH_2	Gamma phase of magnesium hydride (orthorhombic, unstable at high T)	–
α-MgH_2	Alpha phase of magnesium hydride (tetragonal rutile TiO_2 type)	–
Nb_2O_5	Niobium pentoxide catalyst	–
wt%	Weight percent of hydrogen storage capacity	%
T (1 bar)	Equilibrium temperature for MgH_2 decomposition at 1 bar	°C
ΔH	Enthalpy change of reaction	kJ.mol^{-1}
ΔS	Entropy change of reaction	J.(mol.K)$^{-1}$
ΔG	Gibbs free energy	kJ.mol^{-1}
P	Operating hydrogen pressure	bar (or MPa)
P^{eq}	Equilibrium hydrogen pressure	bar (or MPa)
K_{eq}	Equilibrium constant	–
Q_r	Reaction quotient	–
T-desorption	Hydrogen desorption temperature	°C (or K)
ΔG_{nano}	Gibbs free energy at nanoscale (bulk + surface terms)	kJ.mol^{-1}
HCP	Hexagonal close-packed magnesium lattice	–
BCC	Body-centered cubic sublattice	–
V_h	Hydride unit cell volume	Å^3
V_m	Metal unit cell volume	Å^3
R	Universal gas constant (8.314 J.mol^{-1}.K^{-1})	J.(mol.K)$^{-1}$

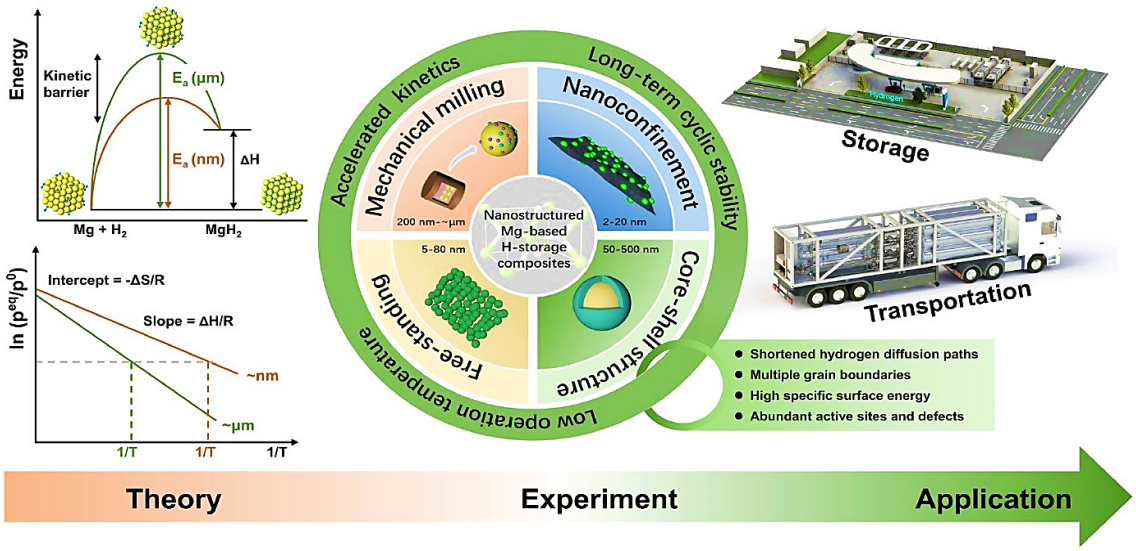

Fig. 2. Schematic illustrations of fundamental theories and strategies for the nanostructures of magnesium-based hydrogen storage materials [6].

The pressure must be released whenever it reaches a certain threshold (roughly 1 MPa) due to the evaporation of liquid hydrogen brought on by the residual thermal leakage. Due to these factors, dense liquid storage has not been widely used, especially in transportation applications. Instead, when boiling is avoided and cost is not an issue, liquid hydrogen is used [23]. Hydrogen storage techniques, such as compressed gas and metallic materials, are gaining popularity due to their low density and short driving distance. These approaches can be classified as physical adsorption using adsorbents and hydrides, in which hydrogen atoms are chemically linked to metal hydrides. These reversible materials may store up to 19% of hydrogen and are classified into two types: physical adsorption with adsorbents and hydrides [24]. Also, in Fig. 3a, you can see different material-based hydrogen storage technologies.

Some materials form a very strong bond when they bond with hydrogen and require very high energy to release the hydrogen. In general, a hydride is a negatively charged anion of hydrogen (H) that has a hydrogen atom with two electrons. Also, all compounds containing H atoms that have a covalent bond and are attached to an element with a lower electronegativity are called hydrides; for example, water (H_2O) is an oxygen hydride, and ammonia is a nitrogen hydride. In such cases, the H center has a nucleophilic character [8].

In general, it is common for two or more metal compounds to form a moderately stable hydride, with one forming an unstable hydride and the other a stable hydride. The order of material desorption is metal > ionic > covalent bonds, which are complex hydrides of an anionic complex with hydrogen covalently linked to a metal or non-metal, such as $(AlH_4)^-$, $(NH_4)^-$, and $(NH_2)^-$. Stronger bonds result in less hydrogen desorption. These materials desorb hydrogen at a much higher temperature [8, 14].

Materials used to store hydrogen include LiH, BeH_2, CaH_2, NaH, and MgH_2. LiH has a weight density of 12.5% but requires temperatures above 700 °C to desorb hydrogen. BeH_2 and AlH_3 have a high weight density but are poisonous and irreversible. CaH_2 and NaH have limited storage capacity but contain less than 5% H_2 by mass [25]. Magnesium hydroxide is the best choice for storing hydrogen due to its low hydrogen desorption temperature, high reversibility, and 7.6% weight density. These materials differ in their ability to store hydrogen [14, 16–20]. Magnesium hydride is a preferred option for storing hydrogen due to its consistent storage density. Because magnesium is inexpensive, stable, non-toxic, and plentiful, it is also used in battery applications other than hydrogen storage.

A solid solution of hydrogen in magnesium (α phase) is formed when hydrogen pressure is applied, as shown in Fig. 3b. This occurs when hydrogen molecules break from the metal surface and hydrogen atoms enter the lattice. The initial α-phase is fully transformed into β-MgH_2 when the hydrogen concentration rises and the β-phase nucleation becomes energetically favorable. Under a hydrogen pressure of roughly 30%, magnesium, which is typically produced as a hexagonal network, expands to form a tetragonal β-MgH_2 structure during the hydrogenation process. At high compressive stress (70–80 bar), β-MgH_2 transforms into the orthorhombic γ-MgH_2 phase. Also, γ-MgH_2 is not stable and returns to tetragonal β-MgH_2 at high temperatures (300 °C) [9, 16, 24, 26].

According to our findings, magnesium has been thoroughly studied for use as a hydrogen storage material due to its abundance, non-toxicity, affordability, and stability. He first examines the basic circumstances and the fundamentals of the Mg-H system before highlighting the most recent advancements in the optimization of magnesium hydride as a hydrogen storage material. Then, the molecular structure of magnesium is investigated, and the factors affecting its thermodynamics and kinetics are pointed out. The scope of magnesium hydride synthesis and its methods are discussed in this review article, which also looks at how to optimize magnesium hydride as a material for storing hydrogen by utilizing different additives, integrating defects, and comprehending rate-limiting processes during adsorption and desorption. Finally, in this article, various characterizations and analyses have been carried out, and various applications of hydrogen and magnesium hydride storage have been mentioned. You can also see the roadmap of this article in Fig. 4.

In the global transition to renewable and sustainable energy systems, hydrogen has become a very appealing energy carrier due to its high

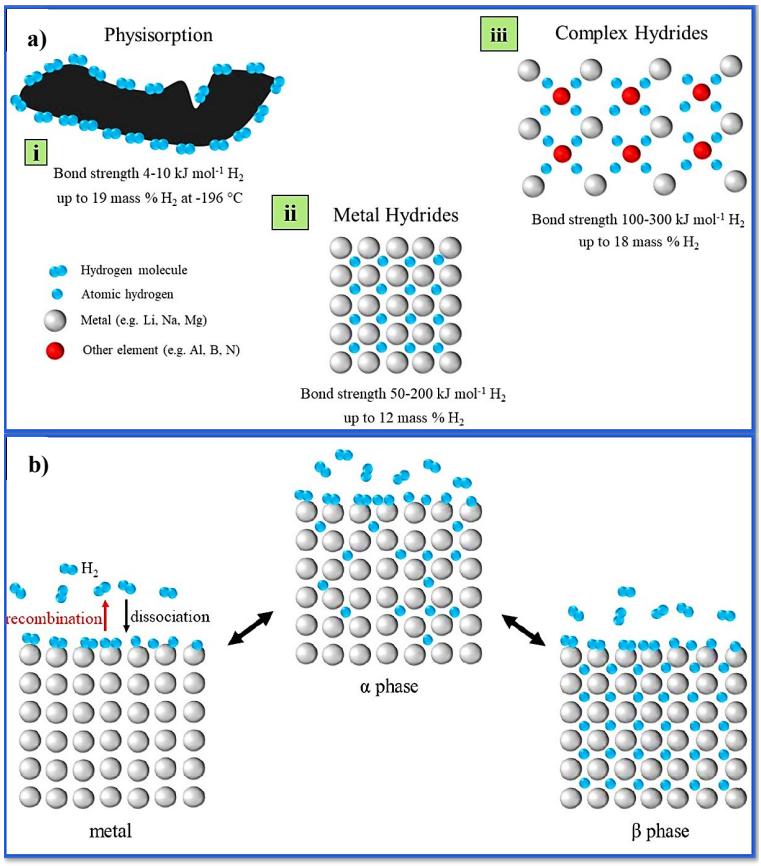

Fig. 3. a) A schematic illustration of various metallic-based hydrogen storage systems, metal hydrides, complex hydrides, and physical absorption of hydrogen [24], and b) schematic representation of the transformation of magnesium into its α and β phases under hydrogen pressure [27].

gravimetric energy density, environmental friendliness, and potential to replace fossil fuels in both stationary and mobile applications. It is attractive due to its natural abundance, relatively low cost when compared to complex hydrides, and exceptionally high potential hydrogen storage capacity of 7.6 weight percent. Despite these advantages, MgH_2 exhibits several intrinsic drawbacks, such as slow hydrogen absorption and desorption kinetics, high enthalpy of formation ($\Delta H \approx 75$ kJ.mol^{-1} H_2), and a high decomposition temperature, typically above 300 °C. These limitations not only hinder fast hydrogen release under practical operating conditions but also pose significant barriers to its integration into next-generation energy systems.

This review seeks to bridge these gaps by conducting a systematic and critical analysis of the advances in MgH_2 research, with a particular emphasis on the dual roles of high-energy reactive ball milling and catalytic doping. Unlike many previous reports that address these modification strategies in isolation, the present study highlights their combined impact on both the thermodynamic and kinetic properties of MgH_2. In doing so, it not only clarifies how ball milling-induced nanostructuring enhances hydrogen diffusion pathways and reduces particle size, but also explains how transition-metal-based catalysts lower activation barriers and promote reversible hydrogen release. Furthermore, the review extends beyond laboratory-scale demonstrations by assessing the scalability and long-term cycling stability of these approaches, thus providing insights that are often overlooked in prior literature.

Ultimately, this study aims to provide a stronger motivation for future research by identifying the shortcomings of earlier investigations and demonstrating how an integrated approach combining mechanical processing, nanostructuring, and catalytic enhancement can accelerate the transition of MgH_2 from a well-studied but problematic hydride to a viable hydrogen storage medium for next-generation energy applications. By offering a comprehensive perspective that interlinks fundamental science with practical engineering considerations, this review aspires to guide researchers toward more targeted, scalable, and application-oriented solutions. In doing so, it lays the foundation for advancing MgH_2-based systems beyond incremental improvements and toward transformative innovations capable of meeting the pressing demands of sustainable hydrogen energy technologies.

2. Basic thermodynamic principles

The behavior and characteristics of MgH_2 are influenced by the thermodynamic analysis of the reaction between Mg and H_2. Due to this, before trying any reaction, it is crucial to comprehend the fundamentals of the magnesium-hydrogen reaction's thermodynamics. MgH_2 is the result of an exothermic reaction between magnesium and hydrogen, which is linked to entropy changes ($\Delta S = -135$ J.mol^{-1}.K^{-1}) of H_2 and enthalpy ($\Delta H = -75$ kJ.mol^{-1}) of H_2 [28].

The driving force behind a process is the Gibbs free energy (ΔG) [28] (Eqs. 3–9), and a reaction is considered thermodynamically favorable when $\Delta G < 0$. This can be written as follows:

$$\Delta G^{\theta} = \Delta H^{\theta} - T\Delta S^{\theta} \quad (3)$$

$$\Delta G^{\theta} = RT \ln K_{eq} \quad (4)$$

$$\Delta G = \Delta G^{\theta} + RT \ln Q_r \quad (5)$$

where Q_r is the reaction coefficient and K_{eq} is the equilibrium constant. The equilibrium constant and the reaction coefficient for the hydrogenation reaction between solid magnesium and H_2 gas are solely dependent on the H_2 pressure and can be written as follows:

$$K_{eq} = \frac{P^{\theta}}{P^{eq}} \quad (6)$$

$$Q_r = \frac{P^{\theta}}{P} \quad (7)$$

in which P is the operating pressure and P^{eq} is the equilibrium pressure. Additionally, the Van't Hoff diagram corresponding to the hydride reaction is illustrated by Eqs. 3–6 as follows.

$$\ln \frac{P^{eq}}{P^{\theta}} = \frac{\Delta H^{\theta}}{RT} - \frac{\Delta S^{\theta}}{R} \quad (8)$$

$$\Delta G = RT \ln \frac{P^{eq}}{P} \quad (9)$$

According to Eq. 9, the conditions necessary for hydrogen storage are determined by the equilibrium pressure of magnesium (P^{eq}). The hydrogenation reaction between magnesium and hydrogen will therefore be thermodynamically beneficial when $P > P^{eq}$ because $\Delta G < 0$. The temperature determines the equilibrium pressure in Eq. 8; therefore, by modifying the temperature, hydrogen absorption and desorption can be regulated [29].

Hydrogen absorption reactions have a corresponding temperature T_0 at pressure P_0, while hydrogen desorption uses a temperature greater than T_0. It is possible to lower the temperature needed for hydrogen emission by altering the system's thermodynamics. Adjusting ΔH^{θ} and ΔS^{θ} correctly can result in lower temperatures T_0 for pressure P_0. Calculations revealed that when the enthalpy varies, the entropy also changes; this phenomenon is commonly referred to as enthalpy-entropy compensation [30, 31].

For a number of hydrogen storage materials, this linear relationship between enthalpy and entropy, which is based on the enthalpy-entropy compensation effect, has been studied. Additionally, when both entropy and enthalpy fall, the temperature at which hydrogen is removed decreases as little as possible. To optimize the drop in desorption temperature, entropy should ideally rise in tandem with the enthalpy decrease [32] (Eqs. 10–15), which is defined as:

$$T_{desorption} = \frac{\Delta H}{\Delta S} \quad (10)$$

Compared to bulk materials, nanoscale particles have a greater surface area, more atoms, and distinct stability and chemical characteristics. The surface energy of bulk materials may typically be disregarded for thermodynamic calculations when they are in the bulk state, but at the nanoscale, the surface energy becomes significant and needs to be taken into account [33]. As a result, an extra surface energy term that can be written as follows is frequently added to the Gibbs free energy for nanosized particles (ΔG_{nano}):

$$\Delta G_{nano} = \Delta G_{bulk} + \Delta G_{surf} \quad (11)$$

where ΔG_{surf} is the extra term resulting from the excess surface energy and ΔG_{bulk} is the Gibbs free energy of the bulk material. The surface energy of a spherical nanoparticle with radius r and molar volume V can be represented as follows:

$$\Delta G_{surf} = \sum_i \frac{3V_i\gamma_i}{r_i} \quad (12)$$

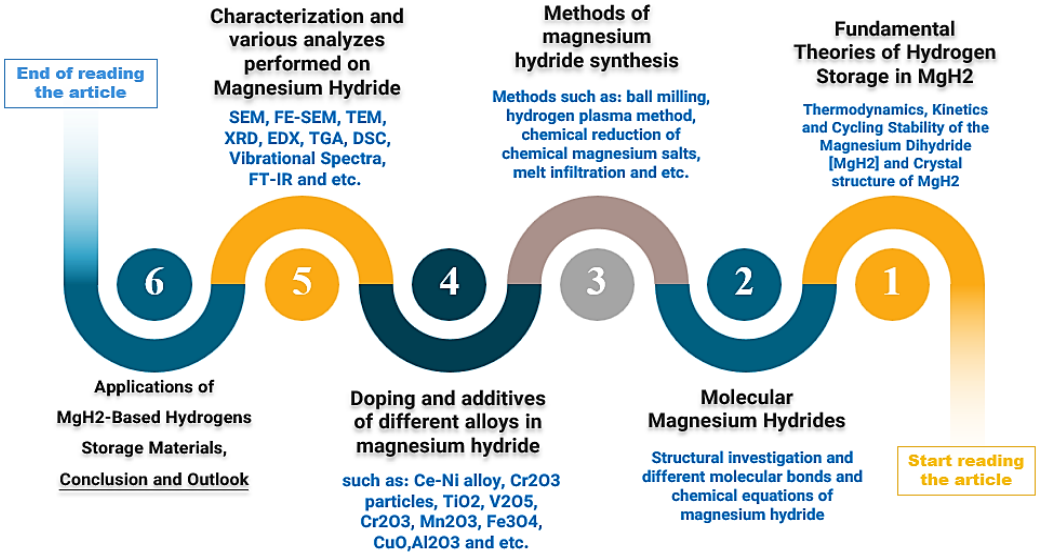

Fig. 4. The road map of this article.

With $\gamma = \delta G/\delta A$ corresponding to the surface energy density on the surface, A can be inserted in the above equation. From Eq. 12, the particle size, molar volume, and surface energy density of the nanosized particles all affect the nanoscale surface energy. A van't Hoff equation for the nanoscale reaction is produced by adding the surface energy term, and it looks like this:

$$\ln P_{nano}^{eq} = \ln P_{bulk}^{eq} + \frac{\Delta G_{surf}}{RT} \quad (13)$$

Then, by substituting Eq. 10 in Eq. 13 for the Van't Hoff equation, we will have:

$$\ln \frac{P_{nano}^{eq}}{P^{\theta}} = \frac{1}{RT}\left(\Delta H^{\theta} + \Delta G_{surf}\right) - \frac{\Delta S^{\theta}}{R} \quad (14)$$

In the case of hydrogen desorption from nanoscale MgH_2, by substituting Eq. 12 into 14, the updated Van't Hoff equation can be written as:

$$\ln \frac{P_{nano}^{eq}}{P^{\theta}} = \frac{1}{RT}\left(\Delta H^{\theta} + \sum_i \frac{3V_i\gamma_i}{r_i}\right) - \frac{\Delta S^{\theta}}{R} \quad (15)$$

The extra surface energy of the nano-sized hydride will therefore result in a lower enthalpy and, consequently, a lower desorption temperature if the surface energy of MgH_2 is higher than that of Mg. For instance, MgH_2 nanoparticles smaller than 4 nm had a lower desorption temperature (253 °C) and a better enthalpy (52 kJ.mol^{-1} H_2) [34, 35].

According to research, MgH_2 nanoparticles should be smaller than 5 nm to facilitate the creation of unstable γ-MgH_2 phases, introduce grain boundaries, and provide extra volume in the deformed areas, all of which improve thermodynamics. It should be mentioned that because of the simplified assumptions used in the computations, computational studies that calculate enthalpy values at the nanoscale may have an error of up to ±20 kJ.mol^{-1} H_2. In the end, the metal hydride nanoparticle model shouldn't produce inaccurate size forecasts because the desired enthalpy for real-world applications is between 20 and 50 kJ.mol^{-1} H_2 [36].

3. Basic kinetics principles

The thermodynamic experimental values of H_2 (ΔH = -74.5 kJ.mol^{-1} and ΔS = -13 kJ.mol^{-1} H_2) indicate that hydrogen desorption processes can occur at 253 °C with 1 bar of pressure offering However, a temperature close to 40 °C is necessary for MgH_2 bulk hydrogen desorption, resulting in a high activation energy barrier (E_a). This process requires both kinetic and thermodynamic control to lower the desorption temperature [36].

The Arrhenius equation can be used to express k(T), which is a general approach to estimate the rate of a reaction at a specific temperature [36].

$$k(T) = Ae^{-\frac{E_a}{RT}} \quad (16)$$

According to the Arrhenius equation, as the activation energy falls, the reaction rate increases. Because of the slow kinetic conditions, bulk magnesium may take many hours to complete the hydration processes [6]. The diffusion rate, the oxide layer covering the magnesium surface, and the low rate of hydrogen dissociation on the magnesium surface are the three main hypotheses offered, though the exact reason for this reaction's slow speed has not yet been determined [37].

Hydrogenation reactions involve a variety of heterogeneous gas-solid interactions with different energy barriers and processes. At the gas-solid interface, hydrogen-surface interactions with magnesium are generally thought to take place at crystallographic defects (such as grain boundaries and surface impurities). Nonetheless, the synthesis of MgH_2 nanoparticles affects the type and amount of defects produced, meaning that it often has a major impact on the kinetics of the reaction. Finding the rate-limiting mechanisms and reducing the related energy barriers are essential to fast kinetics [38].

During the hydration reaction, hydrogen gas is physically adsorbed on the magnesium surface, and H_2 molecules are removed from the surface before the chemical adsorption of H atoms. Physical absorption requires little activation energy and does not slow down kinetics. The dissociation of H_2 molecules into H atoms on the magnesium surface, which has a slightly higher energy barrier of roughly 432 kJ.mol^{-1} H_2,

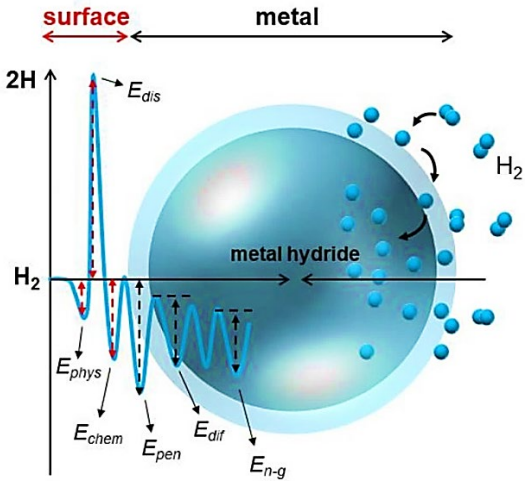

Fig. 5. The Lennard-Jones potential diagram depicts various energy barriers in the metal-hydrogen system at the metal surface and within the metal, such as physical hydrogen adsorption (E_{phys}), H_2 decomposition (E_{dis}), hydrogen chemical adsorption (E_{chem}), hydrogen penetration in the subsurface (E_{pen}), diffusion of H atoms in the bulk (E_{dif}), and nucleation and growth inside the hydride phase (E_{n-g}) [39].

is believed to be one of the primary rate-limiting phases [40]. Magnesium, unlike transition metals like Ni and Pd, lacks d orbitals that can assist H_2 dissociation by interacting with hydrogen bonding orbitals. Furthermore, the oxide layer generated on the magnesium surface promotes weak hydrogen breakdown and chemisorption. This issue is well represented in Fig. 5, which relates to the Lennard-Jones potential diagram for the various energy barriers in the metal-hydrogen system both inside and at the metal surface [39].

H atoms enter through the lower surface and disperse throughout the magnesium matrix once hydrogen has chemically attached to the surface. This additional rate-limiting phase is caused by the low diffusion coefficient of hydrogen in magnesium and magnesium hydride [41]. Next comes the temperature- and pressure-dependent germination and growth phase. Rapid nucleation and development at high temperatures and pressures ($P > P^{eq}$) produce a hydride shell that prevents additional hydration and slows down reaction kinetics. However, the opposite happens at low temperatures and pressures, where the slow diffusion of hydrogen in magnesium becomes the limiting step and hydride phase nucleation occurs inside the magnesium particle without the formation of a hydride shell [42].

Magnesium hydride nanostructures (which reduce the size of magnesium particles to a few nanometers) boost the reaction's kinetics while decreasing its activation energy. The researchers observed that smaller magnesium nanoparticles absorbed hydrogen 7 times faster than 38 nm particles [43].

Increased surface kinks and defects brought on by nanosizing may make the surface more reactive to hydrogen [44]. Other advances in nanosizing include increasing surface area with smaller magnesium nanoparticles, encouraging hydrogen dissociation at the surface, and creating shorter diffusion routes, all of which can speed up hydrogen diffusion. A major energy barrier to diffusion across the hydride is eliminated when nanosizing aids in preventing the formation of a hydride shell. Rather, the last obstacles to magnesium generation are nucleation and growth, which frequently depend on temperature and pressure [45].

When using composites for hydrogen storage based on magnesium, the long-term stability cycle is also crucial. Long-term re-hydrogenation at high temperatures decreases hydrogen storage capacity and the rate of water/hydrogen absorption, according to the experimental results [46]. On the other hand, surface energies stimulate the aggregation and development of nanoparticles, which expands the hydrogen diffusion channel and decreases the kinetics of Mg/MgH_2. In addition to using pure H_2 to prevent capacity loss, the nanoproduct strategy and encapsulation are useful ways for limiting nanoparticle aggregation and growth [47]. The molecular investigation of magnesium hydride nanostructures will be described in depth in the following section.

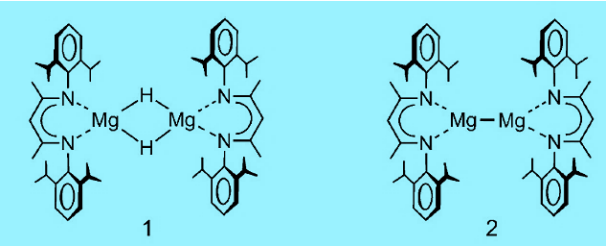

Fig. 6. Schematic of complex 1 and 2 [52].

4. Molecular magnesium hydrides

According to recent thermodynamic simulations, altering the particle size can have some effect on the desorption temperature. The number of surface hydride ions decreases, and the surface-to-volume ratio rapidly increases as MgH_2 particles shrink. For MgH_2 clusters with n<19 (particles smaller than 1.3 nm), this effect is taken into account; for clusters in the sub-nm range, it increases significantly [48, 49].

The breakdown enthalpy is negative (ΔH= -5.5 $kJ.mol^{-1}$) after the linear monomer MgH_2's enthalpy has been calculated. Furthermore, a "bottom-up" molecular approach can be used to create tiny, distinct magnesium hydride clusters from MgH_2 clusters in the sub-nanometer range. By employing a ligand framework, these clusters can subsequently be utilized as the smallest magnesium hydride particles. They are contained and visible. These molecular clusters cannot store hydrogen effectively [49]. However, their molecular composition enables detailed investigation down to the atomic level [48].

Researchers recently described the dimeric magnesium hydride compound β-discriminate (2,6-diisopropylphenyl-nacnac $MgH)_2$ [50]. Because of the steric location of 2,6-diisopropylphenyl (DIPP), the researchers found that this complex is resistant to ligand exchange and the production of the insoluble MgH_2 salt. Because of its stability, β-diketiminate is a promising option for applications involving the storage of hydrogen.

MgI_2 can only be converted to complex 2 by potassium (K) reduction, and complex 1 is thought to be extremely stable (reported disintegration temperature of 300 °C). Nevertheless, hydride complex 1 is not produced when complex 2 is pressurized with H_2 (see Fig. 6). However, oxidation of MgI with AlH_3 resulted in the creation of complex 1 [51]. It seems that more than two metal atoms must work together to directly remove decreasing H_2. Julia et al. discussed their

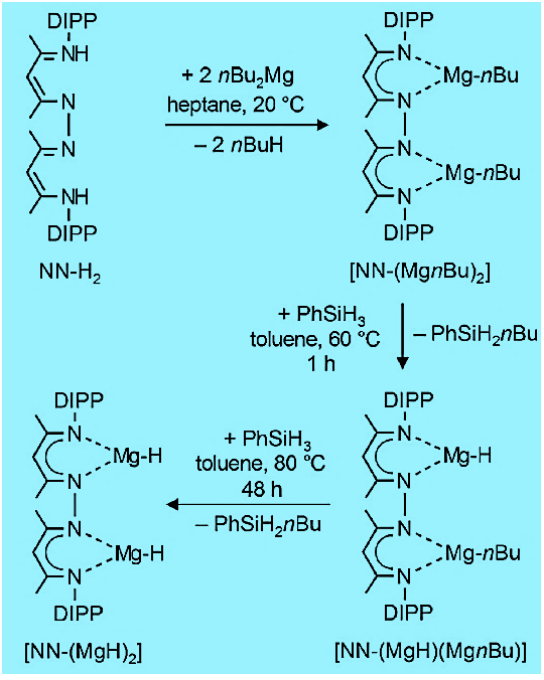

Fig. 7. Schematic molecular process of synthesis (NN-$(MgH)_2$) is proposed in this study [52].

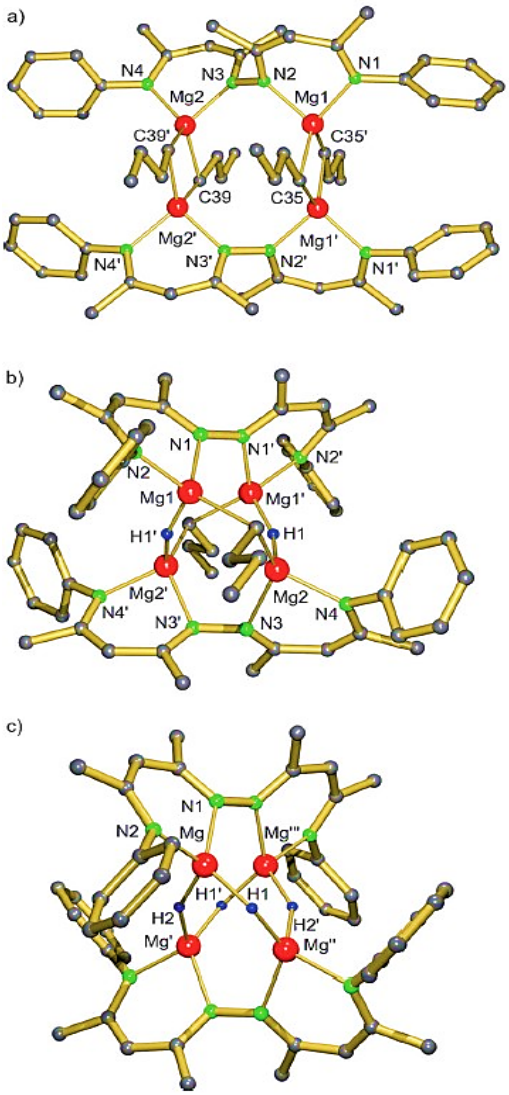

Fig. 8. Schematic of crystal spatial structures: a) crystal structure of (NN-(MgH)$_2$), b) molecular structure of {NN-(MgnBu)(MgH)}$_2$ with a double crystallographic axis, and c) crystal structure of (NN-(MgH)$_2$) with three dual axes of crystallography and crystal system symmetry [52].

research on polymetallic magnesium hydride in this context. According to the study, complex 1 production is significantly decreased when magnesium is alloyed with Ti, V, Cr, Mn, Fe, or Co. [52].

Julia et al. investigated molecular clusters of magnesium hydride and the link between particle size and hydrogen removal temperature. They said that the magnesium hydride complex (NN-(MgH)$_2$) was produced by reacting the NN-H$_2$ ligand with nBu$_2$Mg and then converting two nBu groups into hydrides using PhSiH$_3$. As seen in Fig. 7, the first MgnBu functionality is substantially more responsive than the second. By reacting with PhSiH$_3$ in toluene at 60 °C for an hour, the first nBu anion can be transformed into the hydride; however, the second nBu anion necessitates higher temperatures and longer reaction times (80 °C, 48 hours) [52].

Fig. 8 shows the crystal structure (NN-(MgH)$_2$) with a twofold crystallographic axis placed horizontally in the plane; in (b) the molecular structure of {NN-(MgnBu)(MgH)}$_2$ with a twofold crystallographic axis placed vertically in the projection plane; and in (c) it shows the crystal structure (NN-(MgH)$_2$) where the three crystallographic double axes are perpendicular. Crystals with a yield of 48% were all identified by single-crystal X-ray diffraction. Additionally, Fig. 8 creates a dimer combination where the four Mg^{2+} nuclei are in the same plane. passes through the N-(D$_2$)N bond's center and the H$_1$ and H$_2$ atoms [52].

Solid magnesium hydride (MgH$_2$) has generally been suggested as a material for storing hydrogen. Since the middle of the 20th century, researchers have been interested in soluble magnesium hydride reagents. Over the past 20 years, molecular magnesium hydride chemistry has been introduced by organometallic chemists, who have produced several distinct structural examples. The findings of this study are promising for real-world uses of hydrogen storage technology. These developments could revolutionize the way we store and use energy [8, 30, 53–56].

In 1951, magnesium dihydride (MgH$_2$) was first synthesized by direct hydrogenation of magnesium metal using an MgI$_2$ catalyst at 500 °C and 200 bar H$_2$ pressure [57]. This process was effectively catalyzed by anthracene and intermediate metal halides (Ti, Cr, and Fe) at 658–680 °C and 80 bar H$_2$. The MgH$_2$ (α-MgH$_2$) crystal has Mg-H linkages and a rutile (TiO$_2$) structure at normal pressure. Both β-MgH$_2$ and γ-MgH$_2$ can also develop under high pressure. Additionally, their matrix separation techniques allow the vibrational spectra of a number of molecular forms, such as MgH, MgH$_2$, Mg$_2$H, Mg$_2$H$_2$, Mg$_2$H$_3$, and Mg$_2$H$_4$, to be detected and identified [58, 59].

At room temperature, MgEt$_2$ and LiAlH$_4$ combine to generate microcrystalline magnesium dihydride, also referred to as active magnesium dihydride, which is pyrophoric. Fig. 9 shows the production of activated magnesium dihydride [60].

The equilibrium that causes crystal formation (MgH$_2$) by the corresponding ligand, which is highly sensitive to air and humidity, is one of the challenges [60]. By offering crucial kinetic stability, the proper use of powerful and stable auxiliary ligands, like S-donating, improves the situation. Fig. 10 shows the four distinct reaction types for the currently recognized techniques of magnesium hydride production. The most common, extensive, and advantageous reaction route is generally the Mg-C/H-Si stretching bond metathesis reaction between alkyl magnesium and PhSiH$_3$ [61].

Furthermore, molecular magnesium hydride refers to a variety of MgH$_2$ complexes. The molecular hydrides of group II metals will have comparatively stronger bonds as their size, electropositivity, and lattice energies increase. Additionally, the formation of these compounds depends on the kinetic stability offered by suitable sub-ligands, and the investigated ligands for molecular magnesium hydrides are primarily mono- or di-anionic [60].

The Mg-H bond interaction in MgH$_2$ is primarily ionic, although some covalent character can be seen, in contrast to pure ionic hydrides like LiH. The presence of covalent character in the bond helps explain some of the unique properties of MgH$_2$, such as its ability to reversibly store

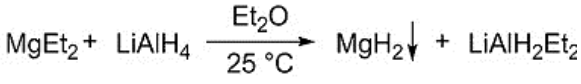

Fig. 9. Synthesis of activated magnesium dihydride [60].

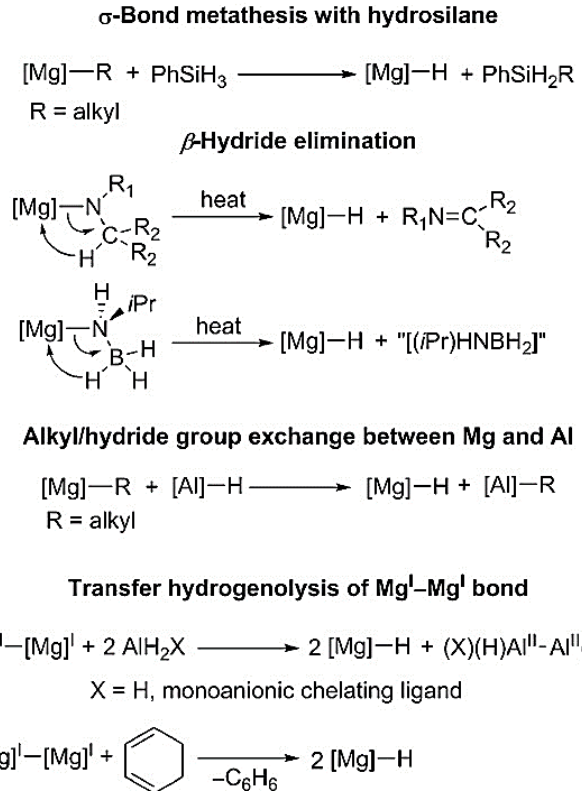

Fig. 10. The main synthetic routes to well-defined molecular magnesium hydrides [60].

hydrogen for use in fuel cell applications. Overall, the combination of ionic and covalent bonding in MgH_2 contributes to its stability and reactivity in various chemical reactions [59].

As a result, the binding energy in MgH_2 is lower than in ionic hydrides like LiH, but it is still considerable when compared to other metal hydrides, such as the much weaker bonding in $LaNi_5H_6$. The addition of another element, such as an intermediary metal, to MgH_2 can help to destabilize it and give it a polymorphic structure due to the Fermi level characteristic. Furthermore, its hydrides are insulating, with a band gap (bandgap energy) of approximately 3–5 eV. This makes them ideal for use as solid-state electrolytes in batteries [59, 62].

5. Mechanisms of absorption and desorption

Now that we have accurately understood the thermodynamic and kinetic relationships in magnesium hydride, as well as its molecular and structural investigation, we may move on to the study of adsorption/desorption and its mechanisms. In general, magnesium's reaction with hydrogen consists of several steps, including physical and chemical absorption, hydrogen diffusion to subsurface and mass network regions, and eventually nucleation and expansion of the hydride phase. During desorption, magnesium must form primary buds, after which hydrogen atoms must go to the subsurface and recombine with hydrogen molecules, causing the transition from the physical to the gas phase. The slowest step in this chemical cycle also determines the overall kinetics of hydrogen absorption [63].

While the hydrogen diffusion constant in magnesium is 10–13 m^2/s in 300 K, the hydrogen diffusion in MgH_2 is at a minimum [64]. As a result, it is envisaged that hydrogenation will gradually slow down following the development of the initial hydride layer around the Mg particles. To determine the rate-limiting phases (kinetic) for both absorption and desorption, they assessed hydrogen absorption and release in a range of samples with very low to high additive concentrations and following very brief to lengthy ball milling times. They discovered that the best fit to their data in the case of absorption was obtained by employing a three-dimensional diffusion-controlled contraction volume model [65] (Eqs. 17 & 18):

$$1-\left(\frac{2\alpha}{3}\right)-\left(1-\alpha\right)^{\frac{2}{3}}=\mathrm{KT} \quad (17)$$

As would be expected from H diffusion through an Mg-hydride layer, this equation best describes the experimental data, where diffusion in the phase transformation is the rate-limiting step. Unlike the absorption and desorption of H_2 from samples that have additives and catalyst content and that require very little grinding time, Bakhrodian et al. [66] obtained the best fit using the limited surface reaction model:

$$\alpha=\mathrm{KT} \quad (18)$$

According to this equation, the primary rate-limiting processes in this process are the recombination of hydrogen atoms and the diffusion from the lower surface to the higher surface.

Moreover, the researchers effectively characterized the thermal desorption spectroscopy results for pure α-MgH_2 using a model of hydrogen evolution from the stoichiometric dihydride during its breakdown [67]. In this concept, the metal phase is first nucleated, and then hydrogen evolves through the surface of the metal islands that are

created (seed nucleation and nucleation). The amount of hydrogen desorption is determined by the final phase, which also serves as a limiting step for the entire process.

In general, the adsorption and desorption mechanisms for magnesium hydride (MgH_2) in hydrogen storage include a series of steps at the atomic level, which are controlled by thermodynamic and kinetic principles. After examining the thermodynamic and kinetic principles as well as the molecular model and its connections, it can be stated that the absorption process includes the absorption of hydrogen gas (H_2) by magnesium (Mg) to form magnesium hydride (MgH_2) (according to Eq. 1) [68]. First, the surface of magnesium particles absorbs hydrogen molecules (H_2). On the magnesium surface, the absorbed hydrogen molecules subsequently split into hydrogen atoms (H) [5]. Of course, this step can be facilitated by the presence of impurities or the use of catalysts [21]. Then the hydrogen atoms are separated and leading to the movement of hydrogen atoms through the magnesium crystal lattice. Finally, the hydrogen atoms find suitable places inside the magnesium lattice and start forming magnesium hydride (MgH_2) buds. These primary buds act as sites of germination [6, 21, 22, 69].

MgH_2 nucleating regions grow by releasing more hydrogen atoms, heating the material, and reacting with magnesium atoms. In the final stage, primary hydrides are formed; this reaction is exothermic and releases heat, leading to the formation of magnesium hydrides [7, 20, 70].

However, the desorption process involves releasing hydrogen gas from magnesium hydride (MgH_2) and returning it to magnesium (Mg). The desorption process requires heating MgH_2 to provide the energy necessary to break the Mg-H bonds. In general, the desorption temperature varies from 300 to 400 °C, which needs to be optimized [21, 22]. Then the supplied thermal energy causes Mg-H bonds to break in magnesium hydride, which is endothermic and absorbs heat [52]. After breaking the bonds, hydrogen atoms diffuse through the MgH_2 matrix on the surface side. Of course, in the presence of existing grain boundaries or catalysts, the diffusion process is facilitated by the microstructure of the material [70]. Finally, the hydrogen atoms on the surface recombine and form hydrogen molecules (H_2) (according to Eq. 2). Also, hydrogen molecules can be released into the surrounding environment as hydrogen gas.

In addition, effective factors affect the process of absorption and resorption and can facilitate the process. In general, the factors affecting these processes are temperature, catalysts, nanoscale, and pressure [5, 15, 21, 22]. Higher temperatures increase the kinetics of adsorption and desorption by providing the necessary energy for hydrogen decomposition, diffusion, and bond breaking. Catalysts such as transition metals (Ni, Pd) can significantly reduce the activation energy for adsorption and desorption, and these processes can be carried out at lower temperatures [15, 22]. Reducing the size of magnesium particles to the nanoscale increases the available surface area for hydrogen interaction, increases the surface-to-volume ratio, and improves the overall kinetics [30]. Finally, high hydrogen pressures increase the speed of the adsorption reaction, while low pressures facilitate the desorption process [7].

6. Methods of magnesium hydride synthesis

The high hydrogen storage capacity and comparatively low cost of magnesium hydride (MgH_2) make it a viable material for hydrogen storage. A number of synthetic techniques have been developed to create MgH_2 with better stability and kinetics. Here, the main methods of magnesium hydride synthesis are described. In general, magnesium hydride (MgH_2) can be synthesized through ball milling (mechanical alloying) [21, 22], thin film deposition [5], electrochemical methods [72], the melt method [55], and high-pressure techniques [73]. In the presence of hydrogen gas, magnesium hydride can also be produced straight from the pure metal [74].

Mechanical alloying is a method of converting alloys into powders of elemental metals without using direct heat. J.S. Benjamin developed this cold alloy process in the 1960s to produce a nickel-based superalloy for gas turbine applications [75]. Mechanical alloying of metal powders involves three processes: cold welding, fracture, and rewelding of the powder particles. These three processes are carried out by the highly powerful impact forces generated by the grinding balls in the mill. From a mixture of elemental or pre-alloyed powders, mechanical alloying effectively creates equilibrium and non-equilibrium alloy phases [76].

Ball milling is conceptually different from mechanical alloying because actual alloying may not occur during ball milling, so particle size reduction is a significant advantage compared to the production of alloys. In general, this effect is suitable for Mg-based nanocomposites because the nanostructure (from ball milling) has been shown in several studies by researchers to improve hydrogen storage properties [21, 22, 24, 77–81]. Furthermore, the high-energy ball milling method can result in the development of solid solutions and amorphous phases, improving the mechanical and chemical properties of the materials. This can result in increased strength, ductility, and corrosion resistance, making ball milling a versatile and valuable approach for developing new materials with specific qualities. Additionally, the final output can be customized to meet the needs of certain applications thanks to the ability to alter milling parameters, including ball-to-powder ratio, speed, and milling duration.

There are different types of ball mills, among which are horizontal ball mills, vibrating ball mills, planetary ball mills, reactive ball mills, and large-diameter ball mills. A variety of large-diameter and abrasive ball mills are used for large-scale sizes (1 to 1000 kg) [76]. Shaker mills and planetary ball mills are more suitable for research purposes due to their ability to handle small amounts of powder [22].

A shaking mill is a very energetic mill that applies motion in three perpendicular directions at more than 1000 rpm. Planetary ball mills are lower-energy mills compared to vibrating mills. The working mechanism of the planetary ball mill consists of a special container that is placed on a rotating disk. During operation, the disc and the vessels (vials) of the mill rotate in opposite directions, and as a result, the centrifugal forces alternately synchronize. This action causes the grinding balls to rise and fall, impacting the materials in the containers [82].

Reactive ball milling (RBM), also known as ball milling in a hydrogen atmosphere, is a useful method for creating a range of hydrides. High mechanical stresses in general can result in high-pressure polymorphism in powders, and the unstable gamma phase of magnesium hydroxide is commonly observed following ball milling. Alloying can be accomplished easily through grinding. Ball milling is the only way to create some alloys, such as iron and magnesium alloys [83].

A high-energy ball mill is now used to describe a rotating cylinder filled with steel or tungsten carbide balls. The balls strike the

magnesium powder, providing the required mechanical energy for the reaction [81]. According to researchers, this process comprises the mechanical grinding of magnesium (Mg) in the presence of hydrogen gas, resulting in the creation of MgH_2 by a combination of mechanical activation and chemical reaction. This approach can result in nanostructured MgH_2 with increased hydrogen storage capabilities. Furthermore, the high-energy ball milling process gives you more control over the size and distribution of particles, resulting in a more consistent and efficient reaction. This approach produces nanostructured MgH_2 with potential hydrogen storage capacity, making it a viable option for clean energy applications. Overall, the combination of mechanical activation and chemical reaction in the high-energy ball milling process has proven to be a successful approach for enhancing the properties of magnesium hydride [24, 77].

Additionally, the researchers said that in order to promote the synthesis of MgH_2, the grinding is carried out in a hydrogen environment [22]. The ratio of pellet mass to powder mass, milling time, temperature, pressure, and speed are some of the variables that affect the milling process. This process is usually done at room temperature, although the process can generate heat that can raise the ambient temperature. Hydrogen gas pressure is also maintained to ensure a continuous supply of hydrogen throughout the milling process [21]. In addition to breaking the oxide layer on the magnesium powder and creating new surfaces, this procedure drastically lowers the size of the powder and grain (crystallite). The size of the required particles and the degree of hydrogenation determine how long the grinding process takes. Another important factor influencing the grinding operation's efficiency is the mass ratio of the pellets to the mass of magnesium powder. Therefore, it is important to carefully control these variables in order to achieve the desired particle size and degree of hydrogenation [21, 22].

The ball milling process causes severe plastic deformation in the magnesium powder, creating defects and increasing the surface-to-volume ratio, which increases the reactivity of magnesium with hydrogen. Repeated collisions and friction between balls and magnesium powder cause hydrogen molecules (H_2) to decompose into hydrogen atoms (H) [24, 82].

In general, a combination of α-MgH_2 and γ-MgH_2 is formed in situ when magnesium metal is ball milled in hydrogen gas, which also lowers the desorption temperature of hydrogen in MgH_2 [84]. In 1990, Fecht et al. began working on the manufacture of nanocrystalline metals using high-energy milling techniques. According to them, ball milling may decrease pure metals with bcc and hexagonal (hcp) crystal structures to 9 nm for bcc metals and 14 nm for hcp metals. [83].

To prevent oxidation, Fecht et al. [83] reacted Zr powder in a steel container with an argon environment for 24 hours. The powder was combined with epoxy, the reaction temperature was kept constant, and a microtome and diamond knife were used to cut thin slices that ranged in size from 20 to 50 nm. Then, Hout et al., inspired by the previous research [83], were able to significantly improve the hydrogen absorption properties of magnesium hydride by using a high-energy ball mill [85]. They concluded that an 18% by weight γ-MgH_2 phase was produced by high-energy ball milling of magnesium hydride at room temperature. The surface of the milled particles was significantly rougher than the unmilled ones, and there was minimal particle aggregation after milling. They also measured the hydrogen desorption temperature, which was reduced to 64 K, using a differential calorimeter. It implies a lower activation energy and quicker hydrogen desorption kinetics [85].

Magnesium hydride is often created when magnesium reacts with hydrogen during milling. Hydrogen can more readily penetrate and react with magnesium as the grinding time increases because the mechanical energy provided to the particles reduces their size, and the specific surface area of the smaller particles enhances the reaction kinetics [86, 87].

Hanada et al.'s study used the mechanical grinding method to examine the connection between magnesium hydride's (MgH_2) nanostructural characteristics and hydrogen storage properties [88]. The MgH_2 nanostructures utilized in this investigation were created by mechanically grinding them in an atmosphere of hydrogen gas. The amount of desorbed hydrogen decreased by 16 weight percent, from 7.3 to 6.1% by weight, during the first two hours of milling. The size of the powder and its crystallites also shrank, and the initial dehydrogenation temperature dropped from 670 K to 70 K. Finally, they discovered that the decrease in crystallite size and lattice strain in MgH_2 during milling has an effect on hydrogen storage capacity. Examining the possible trade-off between greater hydrogen desorption and decreased hydrogen storage capacity is essential when employing mechanical grinding techniques for MgH_2 nanostructures. Furthermore, further investigation is needed to fully comprehend how lattice strain and decreased crystallite size affect the overall capacity to store hydrogen.

High-energy ball mill settings' effects on the microstructure and properties of magnesium hydride and single-walled carbon nanotubes were examined by Kudiyarov et al. Since milling speed and ball milling duration are crucial factors in determining the composite qualities that are created, they were chosen as variable parameters in this study. Fig. 11 displays SEM images of MgH_2-5 weight percentage single-walled carbon nanotube (SWCNT) composites that were acquired after 60 minutes of grinding at 660 and 900 rpm speeds.

In the work of Campos et al., a similar picture with a high concentration of MgH_2 network was seen [89], which can be seen in Fig. 12a. Fig. 12b & 12c also shows the SEM images of the composites obtained by milling at 300 rpm for 120 minutes (a, b) and 180 minutes (d, e) [21].

Physical vapor deposition (PVD) and chemical vapor deposition (CVD) are the two types of thin film deposition techniques that can be used to create doped magnesium-based materials with sizes ranging from a few atoms to micrometers. Materials are evaporated from a solid or liquid source and subsequently deposited on a substrate using the atomic deposition technique known as PVD [90].

In research by Korablov et al. [22], magnesium hydride (MgH_2) was synthesized by ball milling magnesium powder under hydrogen pressure. 202 steel balls with a diameter of 10 mm and a duplex steel container (V = 500 ml) filled with hydrogen gas (P = 24 bar H_2) were used for milling. 400 rpm rotation speed and a 40:1 ball-to-powder mass ratio. For the synthesis, 20.425 grams of magnesium powder were utilized. Ultimately, the produced MgH_2 was combined with 5% by weight of additives to create MgH_2-based nanocomposites. At the same time, magnesium hydrogenation was synthesized using the TiC-2TiB_2 additive. MgH_2-based solutions were ground at 500 rpm for 15 minutes in Ar gas to produce ethylenediaminetetraacetic acid (EDTA) and $AlCl_3$ additions. The produced nanostructures were then ready for examination.

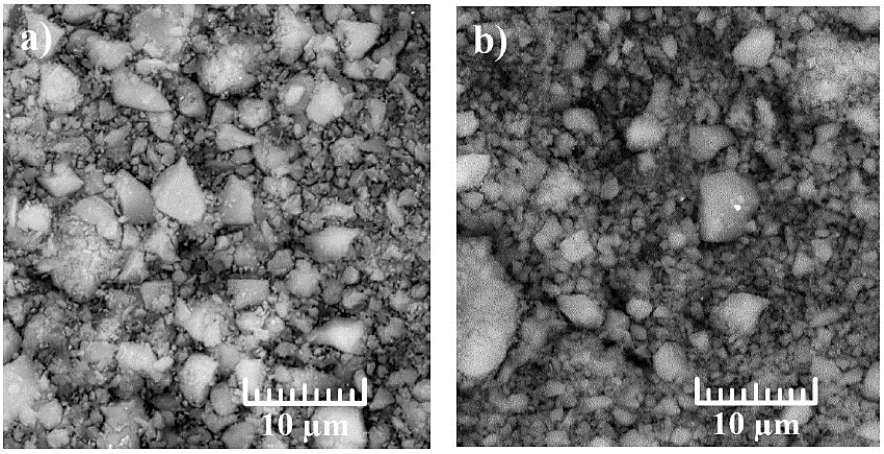

Fig. 11. SEM images of MgH_2-5 wt% after 60 minutes of ball milling with speeds of a) 660 rpm and b) 900 rpm show different morphologies and particle sizes [21].

The milling time required to finish the hydride production process is obviously increased by residual magnesium traces. Additionally, Kurablov et al.'s SEM investigations demonstrated that the nanostructure of the finished product for TiC-2TiB_2-doped magnesium hydride from ball milling occurs [22].

In 2023, research by Zhi-Kang Qin et al. was conducted on hydrogen storage with the synthesis of magnesium hydride. In this research, MgH_2 and $LiBH_4$ were mixed with a weight ratio of 19:1 and subjected to ball milling in a 300 ml tank. A planetary ball mill was used to mechanically mill one gram of mixed material in a grinding tank for ten hours at 400 rpm. Twenty 30-minute intervals were used to mill all of the prepared samples, with a 2-minute break in between. Additionally, pure MgH_2 doped with 5 weight percent $Li_2B_{12}H_{12}$ [4].

Since $LiBH_4$ acts as an ionic conductor to increase the grinding kinetics in MgH_2, the researchers performed it with pure MgH_2 systems doped with $Li_2B_{12}H_{12,}$ and in Fig. 13, the adsorption and desorption kinetics of pure hydrogen doped with $Li_2B_{12}H_{12}$ and MgH_2 doped It is done with $LiBH_4$ at a temperature of 300 °C. As shown in Fig. 13a, MgH_2 has poor kinetics for hydrogen desorption; in 40 minutes, less than 0.7 weight percent of hydrogen is desorbed. However, the kinetics of MgH_2 desorption are enhanced by the presence of complicated borohydrides [4].

Dehydrogenation can be completed rapidly, releasing 1.7 wt% of hydrogen within 40 min, which represents a tenfold increase compared to pure MgH_2. A similar increase in desorption was observed in the MgH_2 system doped with $Li_2B_{12}H_{12}$. Fig. 13b also shows that MgH_2 doped with $LiBH_4$ has hydrogen adsorption kinetic properties [4].

6.1. Magnesium-based hydrogen storage materials: recent developments

The impact of newly developed techniques, such as mechanical ball milling, methanol-wrapped chemical vapor deposition (MWCVD), plasma-assisted ball milling, and organic ligand-assisted synthesis, on hydrogen storage performance was highlighted by Xu et al. and associates in their comprehensive analysis of recent advancements in the production processes of magnesium-based hydrogen storage materials. Their research indicates that while MWCVD and organic ligand-assisted techniques offer high-performance materials with controllable nanostructures, their scalability is constrained. On the other hand, due to their affordability and scalability, mechanical ball

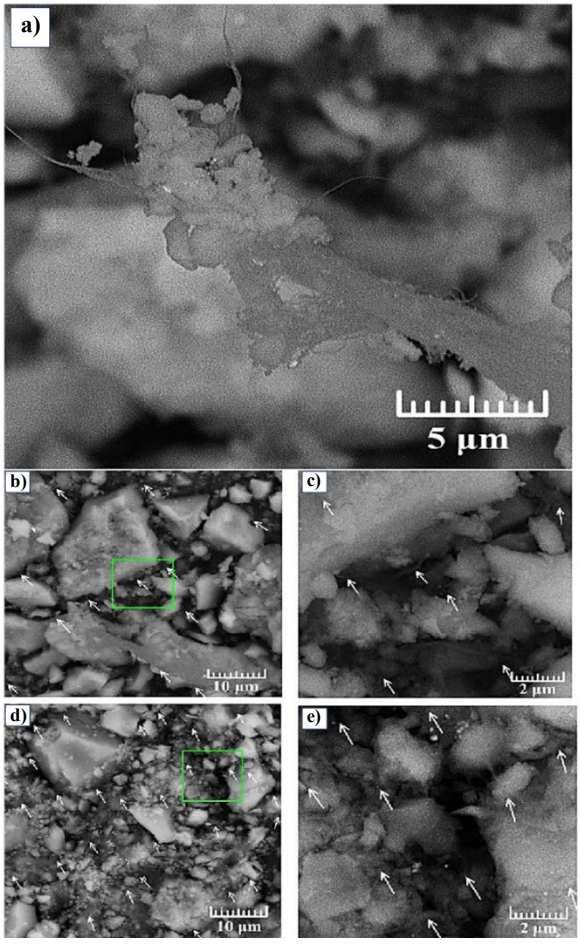

Fig. 12. a) SEM image of magnesium hydride nanocrystals, b, c) SEM images of MgH_2-5 wt% multi-walled carbon nanotube (MWCNT) composite with 120 rpm, and d, e) 180 rpm [21].

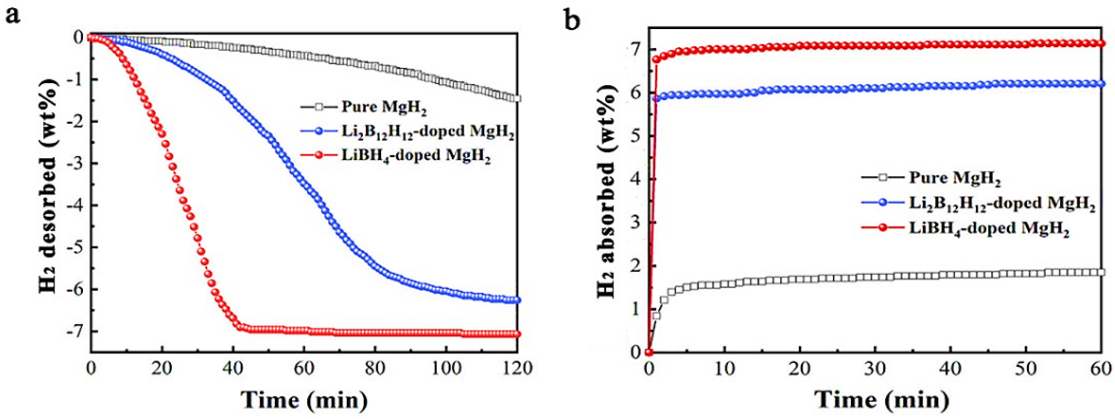

Fig. 13. Graphs of a) hydrogen desorption and b) adsorption kinetic curves of net, $Li_2B_{12}H_{12}$-doped and $LiBH_4$-doped MgH_2 at 300 °C [4].

milling and plasma-assisted ball milling are the most promising methods for practical use. The study emphasized that hydrogen storage capacity and kinetics remain critical challenges [91].

Theoretically, MgH_2 has a storage capacity of 7.6 weight percent; however, contaminants, surface oxidation, and incomplete hydrogenation make practical values less feasible. Rapid hydrogen absorption and release are restricted by slow solid-state diffusion and high activation energy barriers for hydrogen dissociation and recombination. According to Xu et al., sorption kinetics can be greatly improved by using catalytic additions (such as metal oxides, bimetallic alloys, and metal-organic frameworks) and nanostructuring techniques that lower energy barriers and increase diffusion rates. The review also focused on cycling stability. Magnesium-based materials tend to degrade during repeated hydrogen absorption-desorption cycles due to particle agglomeration, surface oxidation, and phase segregation, which reduce specific surface area and reactivity [91].

The authors suggested that the combination of nanostructuring and catalytic doping can mitigate these degradation mechanisms, improving long-term reversibility and performance. In their conclusion, Xu et al. presented several research directions, including the development of novel catalytic systems, the rational design of materials based on magnesium nanostructure, multi-scale computational modeling, the exploration of combined preparation methods (ball milling + MWCVD), system integration optimization, and the development of scalable production and recycling strategies. These strategies aim to develop magnesium-based hydrogen storage materials that are safe, effective, and affordable for practical hydrogen energy applications [91].

Xu et al. investigated the development of magnesium-based hydrogen storage materials using mechanical ball milling as a versatile and scalable technique. Ball milling, they pointed out, allows MgH_2 to be homogenized and nanostructured, which greatly enhances the kinetics of hydrogen absorption and desorption and lowers reaction temperatures without the need for external heating. The study emphasizes that optimization of milling parameters, including milling time, speed, and energy input, is crucial to achieving high hydrogen storage capacity, fast kinetics, and reproducible performance for both laboratory-scale and industrial-scale production. The authors also examined the effect of catalytic additives such as transition metals, metal oxides, carbon materials, and metal halides, showing that these additives enhance hydrogen sorption kinetics by facilitating hydrogen dissociation, diffusion, and recombination [92].

Furthermore, the review discussed nanocomposite strategies, including the combination of Mg-based hydrides with MOFs, other hydrides, and carbon scaffolds, which improve performance via nanoconfinement and interfacial effects. Structure–property correlations and synergistic mechanisms were clarified by using advanced characterization techniques, including XRD, TEM, XPS, and Raman spectroscopy, in conjunction with theoretical tools like DFT and molecular dynamics. Despite these advancements, Xu et al. pointed out persistent challenges: (1) the hydrogen storage capacity remains below the theoretical limit due to impurities and oxidation, (2) low-temperature kinetics (<100 °C) are still insufficient for practical on-board storage, (3) cycling stability is limited by sintering, coarsening, and structural degradation, (4) safety and material compatibility need further investigation, and (5) cost and scalability of ball milling processes require optimization [92].

The authors recommended several approaches for future research to address these issues, including the development of new magnesium-based alloys and composites, advanced ball milling techniques (such as planetary and attritor mills), multi-scale characterization and modeling, nanoconfinement and catalysis methods, and the integration of magnesium-based hydrides into prototype hydrogen storage systems. Overall, Xu et al. demonstrated that ball milling innovations provide a solid foundation for practical Mg-based hydrogen storage applications, offering enhanced kinetics, cycle stability, and scalability, while highlighting areas for further improvement to meet the demands of hydrogen energy technologies [92].

Soltani et al. developed a $ZnSnO_3$–SnO_2 nanocomposite as an efficient catalyst for hydrogen generation via sodium borohydride ($NaBH_4$) methanolysis. They used a modified sol-gel technique, which is new in this field, combining zinc acetate and tin chloride with EDTA ammonium salt as an electrosteric stabilizing and chelating agent. Characterization of the synthesized nanocomposite was done with TGA/DSC, XRD, FTIR, UV-Vis spectroscopy, and SEM. XRD analysis indicated an average crystalline size of 32 nm, while SEM images showed that SnO_2 nanoparticles were deposited on $ZnSnO_3$ aggregates of 10–50 μm [93].

The combination of $ZnSnO_3$ and SnO_2 exhibited significant catalytic activity. A total of 374.11 $ml.min^{-1}.g^{-1}$ (832.38 h^{-1}) was reported as the

TOF. The activation energy was 43.19 kJ.mol^{-1}, the enthalpy ΔH was 40.65 kJ.mol^{-1}, and the entropy ΔS was -178.96 J.mol^{-1}.K^{-1}. Moreover, the catalyst retained 87% of its activity after four cycles, demonstrating excellent stability and recyclability. These findings suggest that the $ZnSnO_3$–SnO_2 nanocomposite is an economical, environmentally friendly, and effective catalyst for hydrogen production. The study highlights the importance of nanostructuring, chelating agents, and composite formation in improving the efficiency, stability, and reusability of hydrogen production catalysts, offering valuable insights for future development of advanced catalytic systems in sustainable hydrogen generation [93].

Recent developments in materials for hydrogen synthesis and storage based on magnesium and zinc have shown great promise for real-world uses. Xu et al. comprehensively reviewed various preparation methods for Mg-based hydrogen storage materials, including mechanical ball milling, methanol-wrapped chemical vapor deposition, and plasma-assisted techniques, highlighting strategies to improve hydrogen capacity, kinetics, and cycling stability. In a complementary study, Xu et al. focused on ball milling innovations, showing that optimization of milling parameters and incorporation of catalytic additives or nanocomposites can significantly enhance the hydrogen absorption/desorption performance and scalability of MgH_2-based materials. Expanding beyond storage, Soltani et al. demonstrated that a $ZnSnO_3$–SnO_2 nanocomposite synthesized via a modified sol-gel method with EDTA ammonium salt as a chelating agent can efficiently catalyze hydrogen production from sodium borohydride methanolysis, achieving high turnover frequency, low activation energy, and excellent recyclability.

6.2. Cost-effectiveness and long-term cycling stability of MgH_2

While laboratory-scale improvements in Mg-based hydrogen storage materials have demonstrated remarkable enhancements in kinetics and capacity, translating these advances to industrial-scale applications requires careful consideration of cost-effectiveness. Synthesis techniques, including reactive milling, methanol-wrapped chemical vapor deposition (MWCVD), and high-energy ball milling, may need expensive precursors, specialized equipment, or significant energy consumption, which may restrict their economic viability. Recent studies, however, have begun to address these economic constraints by optimizing milling parameters, reducing catalyst loadings, and developing scalable mechanochemical methods. For example, Xu et al. demonstrated the production of MgH_2-based composites with fast hydrogen absorption/desorption kinetics using an attritor-type ball mill, achieving high throughput while maintaining relatively low energy input and material costs. By carefully balancing performance with production efficiency, these approaches illustrate pathways to economically viable Mg-based hydrogen storage solutions [91, 92].

Long-term cycling stability remains a key factor in the practical use of magnesium-based hydrides. Phase segregation, surface oxidation, particle coarsening, and loss of active surface area are common outcomes of frequent cycles of hydrogen absorption and desorption, all of which progressively reduce the effectiveness of hydrogen storage. Empirical evidence shows that even high-performance nanostructured MgH_2 composites can experience significant capacity loss after several hundred cycles if protective strategies are not implemented. Therefore, understanding and mitigating degradation mechanisms is central to ensuring reliable operation under realistic conditions.

To enhance cycling stability, several advanced strategies have been explored. Confining nanoparticles in porous scaffolds, encapsulation with carbon-based materials, and introduction of anti-sintering additives have been effective in maintaining particle size and surface area during extended cycling. Catalytic additives, such as Ti- and Nb-based compounds, not only improve hydrogen kinetics but also contribute to structural stability by facilitating reversible phase transformations and preventing irreversible agglomeration. Studies by Xu et al. and Zhou et al. reported that MgH_2 composites combined with carbon nanofibers or MOFs retained more than 85–90% of their initial hydrogen capacity after 50–100 cycles, demonstrating that tailored nanostructuring and composite design are key to long-term performance [5, 91, 92, 94].

A comprehensive framework for moving magnesium-based hydrogen storage toward practical applications is provided by including cost-effectiveness and cycling stability factors into material design. By optimizing synthesis techniques for both scalability and economic feasibility, while simultaneously applying structural stabilization strategies, researchers can develop Mg-based hydrides that balance high capacity, fast kinetics, and durability. Furthermore, integrating these materials into prototype storage systems allows for realistic performance evaluations, including thermal management, pressure cycling, and safety assessments. Collectively, these efforts indicate that Mg-based hydrogen storage can move beyond laboratory demonstrations to practical, long-term, and economically viable energy solutions [5, 92].

In summary, addressing cost-effectiveness and long-term cycling stability is essential for the practical deployment of magnesium-based hydrogen storage materials. While laboratory-scale methods have enhanced hydrogen capacity and kinetics, scalable and economically viable synthesis routes such as optimized ball milling and mechanochemical approaches are critical for industrial applications. During repeated cycles of hydrogen absorption and desorption, structural stabilizing techniques such as carbon encapsulation, nanoconfinement, and catalytic additives successfully reduce deterioration.

Overall, cost considerations and long-term cycling stability are just as important as enhancing hydrogen capacity and kinetics for the practical application of magnesium-based hydrogen storage materials. Alloying, catalytic improvements, and the application of scalable ball-milling processes are examples of recent developments that have shown promise in lowering manufacturing costs without sacrificing performance. Moreover, strategies such as nanoconfinement, carbon coating, and optimized catalyst distribution help preserve the structural integrity of Mg-based hydrides over extended hydrogen absorption/desorption cycles. These combined approaches offer a path toward the creation of sustainable and commercially feasible magnesium-based hydrogen storage devices by taking durability and economic factors into account [5].

6.3. Heat management in MgH_2 hydrogen storage tanks: heat exchangers and thermal control

The impacts of pulsed heating on MgH_2 desorption kinetics and thermal efficiency in solid-state hydrogen storage were investigated numerically by Lanbaran et al. [95]. They used a pulsed (ON/OFF) heating technique to improve the hydrogen release performance of MgH_2. They demonstrated that a 15-minute pulsed heating cycle could

reduce the desorption time by 25%, achieving complete hydrogen release in 45 minutes, while maintaining efficient desorption kinetics and improved thermal management. The study offers crucial insights into the processes of mass and heat transport under pulsed heating and suggests reactor layouts that are optimum for realistic hydrogen storage applications [95].

The authors assessed and contrasted two heating strategies, constant radial heat flux and stepwise pulsed heat flow, in a 2D symmetric geometry using finite element simulations in COMSOL Multiphysics (Fig. 14). This figure, which can be included in our review, schematically represents the MgH_2 tank setup: (a) the traditional method with continuous uniform heating, and (b) the pulsed heating approach where the external wall alternates between ON and OFF states. In terms of thermal efficiency and hydrogen desorption management, the graphic shows how pulsed heating clearly outperforms traditional constant heating by enabling accumulated heat to enter the MgH_2 bed more deeply without overheating the wall [95].

In order to improve thermal conductivity by almost an order of magnitude, a critical component of precise heat-transfer modeling, the simulated bed in the approach was made of MgH_2 mechanically combined with 8 weight percent expanded natural graphite (ENG). Realistic boundary characteristics like fixed surfaces, conductive heat transfer borders, and hydrogen gas outlet paths were incorporated into the models. To enable useful comparisons between the two approaches, important factors such as the initial temperature, hydrogen gas flow rate, and heat flux intensity were maintained constant. The results show that the pulsed heating approach improves both desorption kinetics and thermal efficiency, providing a numerical basis for designing more efficient and practical MgH_2-based hydrogen storage systems.

Overall, the study by Davoud Abdi Lanbaran et al. demonstrates that pulsed heating offers significant advantages over conventional continuous heating for MgH_2 hydrogen storage. Their numerical simulations show that the pulsed (ON/OFF) approach accelerates hydrogen desorption, enhances heat penetration, and improves thermal efficiency, providing key insights for the design of more effective and practical solid-state hydrogen storage systems.

7. Various additives in magnesium hydride

In storage applications, high temperatures are often viewed as a drawback. Numerous studies have been conducted to enhance MgH_2's thermodynamic properties. One solution is to use additives and change the reaction equilibrium [96]. Compounds that form magnesium alloys, such as Al-Mg, or additives that form ternary hydrides and decrease the reaction enthalpy, such as Mg_2NiH_4 [97]. Of course, the enthalpy values of these hydrides are still high and are in the range of 60 kJ/mol. According to theoretical calculations, MgH_2 atomic clusters that contain a small number of atoms have less thermodynamic stability [98].

However, the experimental results showed that even in these atomic clusters, the thermodynamic equilibrium changes are very small, and this is because small positive values for enthalpy are neutralized by small positive values for entropy [2]. Magnesium hydride's slow

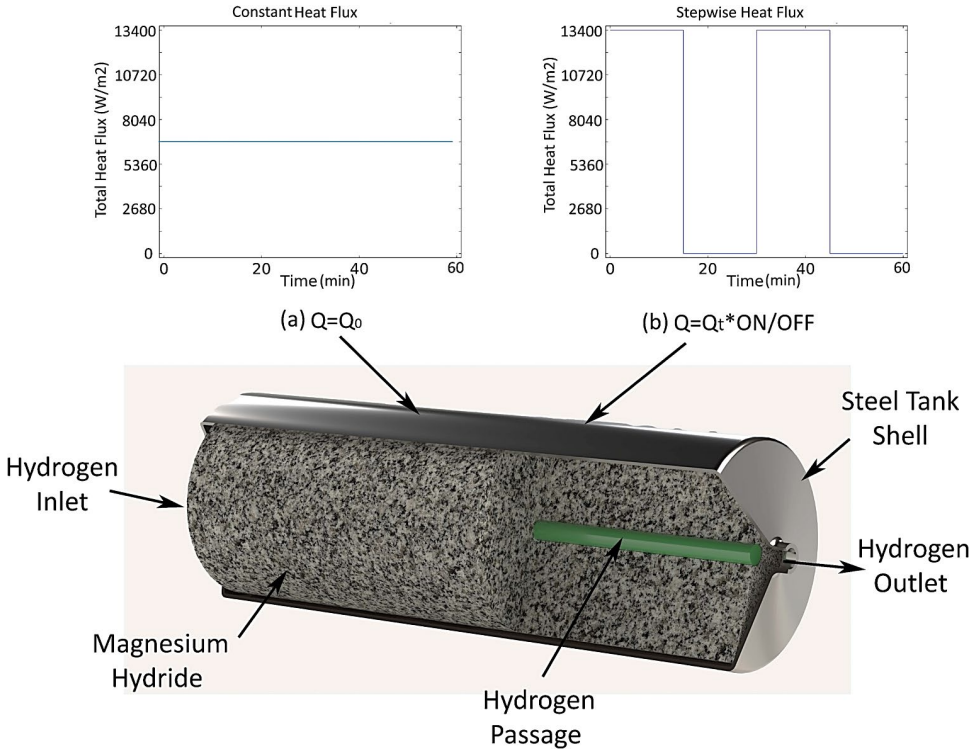

Fig. 14. Schematic of the MgH_2 tank showing a) continuous heating and b) pulsed (ON/OFF) heating. Pulsed heating improves heat penetration, desorption kinetics, and thermal efficiency [95].

kinetics of hydrogen absorption and desorption processes are another problem. It is possible to alter kinetic characteristics by altering the size of magnesium particles. Particle kinetics are greatly enhanced when particle sizes are reduced to the nanometer range. The decrease in the hydrogen atom's penetration path in the solid state and the increase in the surface-to-volume ratio of the particles are the causes of this phenomenon [99]. Several methods have been investigated for the synthesis of nanostructured magnesium hydride. Asianizing MgH_2 micron powder, along with some catalyst, is often a suitable method. For example, metals such as Pd and Ni or metal oxides such as N_2O_5 have an optical effect [100].

In MgH_2 grinding, multi-walled carbon nanotubes improve the kinetics of hydrogen release, releasing 5% weight of the stored hydrogen in the first five minutes. On the other hand, grain expansion brought on by high temperatures diminishes efficiency and kinetic characteristics. Capture nanoparticles in porous supports with particular surfaces, large pore volumes, and chemical neutrality to stop grain growth. Carbon-based materials can be used to facilitate the synthesis of nanoparticles of magnesium hydride [2, 101–104].

Magnesium particles can also be synthesized at temperatures lower than the melting point of Mg. In this method, magnesium atoms are evaporated during heating in a neutral atmosphere and deposited on the surfaces and holes of the support through the penetration mechanism [105]. It is predicted that small MgH_2 nanoparticles can be synthesized by the vapor infiltration method on porous carbons, and nanocomposites with controlled particle size can be prepared. In addition, the resulting materials would have potential applications in hydrogen storage.

Danaei et al. [106] compared hydrogen desorption from unmilled and milled magnesium hydride for 33 min and found that milling can reduce the onset temperature of desorption to about 45 °C. Shang et al. [107] investigated the desorption temperature of magnesium hydride at different milling times and showed that milling for 8 and 15 hours reduced the desorption onset temperature to 73 and 83 °C, respectively.

Hanada et al. [108] showed that the combination of magnesium hydride and niobium oxide milled for 15 minutes has two peaks in the desorption graph at temperatures of 233 and 273 °C. After milling for 2 hours, they saw a decrease in the peak that exists at a higher temperature. And milling for 23 hours also leads to only one peak at about 233 °C. When Simchi et al. [109] investigated the desorption temperature of magnesium hydride at various milling times, they discovered that the temperature decreased as the milling time increased up to 4 hours and increased as the milling time increased beyond 4 hours.

Barkhordarian et al. [66] investigated the desorption kinetics of 3% wt niobium oxide in different times of magnesium hydride with 1% milling and showed that the desorption reaction speed improved by 133 hours compared to 2 hours. Fuster et al. [110] indicated that the reduction of the magnesium dehydrogenation temperature was a result of milling the magnesium particles for a length of 7 to 133 hours. In order to increase the specific surface area and facilitate more collisions between the metal and improver particles, grinding reduces the size of the particles and creates voids and fractures on their surface. This accelerates the reaction, lowers the desorption temperature, and facilitates the penetration path of hydrogen atoms. It reduces the surface of the metal, but with an excessive increase in the grinding time, this effect may be lost by creating a lumpy state in the particles and leading to an increase in the desorption temperature. This can result in decreased hydrogen storage capacity.

Magnesium hydride removal behavior has been improved by a variety of additions with varying effects, which are assessed in two oxide and non-oxide portions. In the section on oxide additives, Barkhordarian et al. showed that a magnesium nanocrystal with 0.2 mol% Nb_2O_5 has better hydrogen absorption kinetics compared to the same amount of Cr_2O_3, and Fe_3O_4 shows a much lower effect than Cr_2O_3 under the same test conditions. Additionally, they investigated how various concentrations of niobium oxide affected the desorption behavior and discovered that greater improver concentrations improved the desorption kinetics, reaching the ideal limit of 0.5 mol% improver [28].

From the research of Huhn et al. [111], it can be seen that the addition of 5% Nb_2O_5 greatly improves the speed of the desorption reaction. Friedrichs et al. [112] showed that the combination of MgH_2 with 2 mol% Nb_2O_5 released 6.4% of hydrogen in 114 seconds, while magnesium hydride alone released 7.6% of hydrogen by weight in 114 seconds. The time is 114 seconds.

Polanski et al. [113] investigated the effect of chromium, iron, titanium, zinc, and indium oxides on magnesium hydride desorption rate. The results showed that Cr_2O_3 and then TiO_2 have the greatest effect on increasing the rate of hydrogen desorption. In addition to causing or increasing surface imperfections on magnesium hydride during grinding, metal oxides with tiny and hard particles also aid in accelerating the desorption reaction by exchanging electrons with hydrogen. Among these additives, Nb_2O_5 has the greatest effect on the speed of the magnesium hydride absorption reaction.

However, in the non-oxide additives section, Veron et al. [114] investigated the desorption behavior of magnesium hydride in the presence of multi-walled carbon nanotubes and cobalt, and according to the results, they found that the effect of cobalt on reducing the desorption temperature is better than the effect of multi-walled carbon nanotubes, but the simultaneous addition of carbon nanotubes Multi-walls and cobalt have a much better and stronger effect on reducing the temperature and absorption. According to the findings of Ranjbar et al. [115]. The use of silicon carbide improver reduces the desorption temperature of magnesium hydride by 23 °C, and if silicon carbide is used together with nickel, this temperature reduction reaches 83 °C. Jin et al. [116] showed that among metal fluorides, Ni, Ti, V, and Nb fluorides have a greater effect on reducing the dehydrogenation temperature of magnesium than Cr, Zr, and Fe fluorides. Czujko et al. [117] applied a different light hydride, such as lithium allanate, to lower the desorption temperature of magnesium hydride. They found that by lowering the activation energy of the desorption reaction, increasing the weight percentage of lithium allanate lowers the dehydrogenation temperature of magnesium. When magnesium hydride was mixed with 3 weight percent lithium allanate, the dehydrogenation temperature was observed to drop by around.

The kinetics of hydrogen desorption were found to be significantly improved when Wu et al. [118] examined the catalytic effect of 5% by weight of various carbon materials, such as graphite, activated carbon, carbon black, and single-walled carbon nanotubes, on the rate of magnesium hydride desorption reaction. The strongest effect was seen in carbon nanotubes with a single wall. In their study, Gasan et al. [119] examined the impact of adding 5% by weight of graphite, V, Nb, and Ti additives on the hydrogen desorption temperature from magnesium hydride. They found that these improvers raised the temperature to 383.9, 376.3, and 384.7, respectively, and

decreased 373.1 °C. In contrast, they reported that the desorption temperature of magnesium hydride milled without additives was 421 °C.

By decreasing the activation energy barrier and shifting the rate-limiting phase from the nucleation and development of magnesium metal to hydrogen atoms to the surface and producing hydrogen molecules, non-oxidative improvers generally aid in lowering the desorption temperature and speeding up the reaction. Also, these materials, with their hard nature, cause holes and porosity in magnesium hydride during grinding and thereby shorten the path of hydrogen penetration. Also, some improvers play the role of a lubricant during grinding. In addition, Table 3 shows the desorption temperature of magnesium hydride in the presence of different improvers. Of course, it should be noted that the different conditions of the test, which include grinding time and speed, particle size, initial desorption temperature, and operating pressure, also affect the desorption temperature. Therefore, a thorough understanding of these variables is crucial for accurately predicting the desorption temperature.

By adding Ti and other elements to Mg by PVD procedures, the Mg-Ti-H system is created, which may have an impact on MgH_2 stability. The thin films of Mg-Ni-Ti ternary alloys produced by Gremaud et al. [121] demonstrated a decrease in the hydrogen adsorption/desorption enthalpy to 40 kJ/mol^{-1} H_2, as illustrated in Fig. 15. The Ni and Ti included in the magnesium alloy are the cause of this drop in enthalpy.

Chemical reactions can be used to create MgH_2 and doped magnesium-based hydrides from organic molecules. One of the bottom-up methods for creating magnesium-based nanoparticles is chemical reduction, which has a number of benefits, such as facile isolation, stable nanoparticles, morphological control, and simplicity of scale-up [122].

Magnesium hydride's molecular chemistry has been thoroughly studied by researchers over the last 20 years, using several well-characterized structural examples [123]. Norberg et al. [43] mentioned that low-temperature reduction increases the density of defect sites in magnesium nanocrystals, offering a straightforward method to significantly boost the rate of H_2 uptake kinetics.

Table 3. Comparison of the effect of non-oxidizing improvers on the reduction of temperature and hydrogen absorption from magnesium hydride.

Enhancer (additives)		Desorption temperature (°C)	Ref.
Type	Value		
NI	5 mol%	260	[108]
Co	5 wt%	325	[115]
V	5 wt%	3.376	[119]
Nb	5 wt%	7.384	[119]
Ti	5 wt%	1.370	[119]
G	5 wt%	9.383	[119]
NiF_2	1 mol%	260	[117]
TiF_3	1 mol%	260	[117]
VF_4	1 mol%	260	[117]
NbF_5	1 mol%	260	[117]
FeF_2	1 mol%	275	[117]
CrF_2	1 mol%	280	[117]
SiC	5 wt%	390	[116]
$LiAlH_4$	10 wt%	355	[118]
SWCNT	5 wt%	325	[21]
MWCNT	5 wt%	350	[120]

hydrogenation in light of this knowledge of the hydrogen reaction in the metal-hydrogen system: (1) H_2 molecules physically absorb, (2) H_2 molecules dissociate, (3) H atoms penetrate the surface, (4) H atoms emit in the lattice, and (5) hydride production occurs at the metal/hydrogen interface, as demonstrated in Fig. 16. The five steps are crucial for the successful conversion of Mg-based systems to hydrogenation.

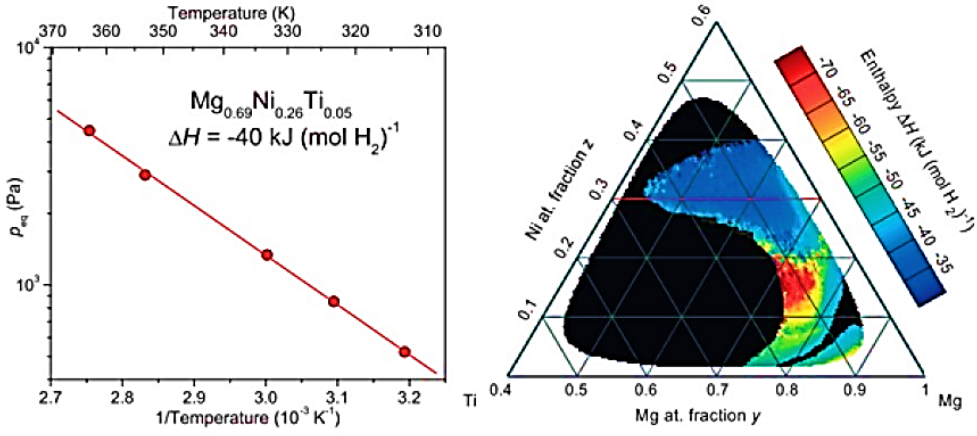

Fig. 15. Enthalpy change diagram of a thin layer of Mg-Ti-H system [121].

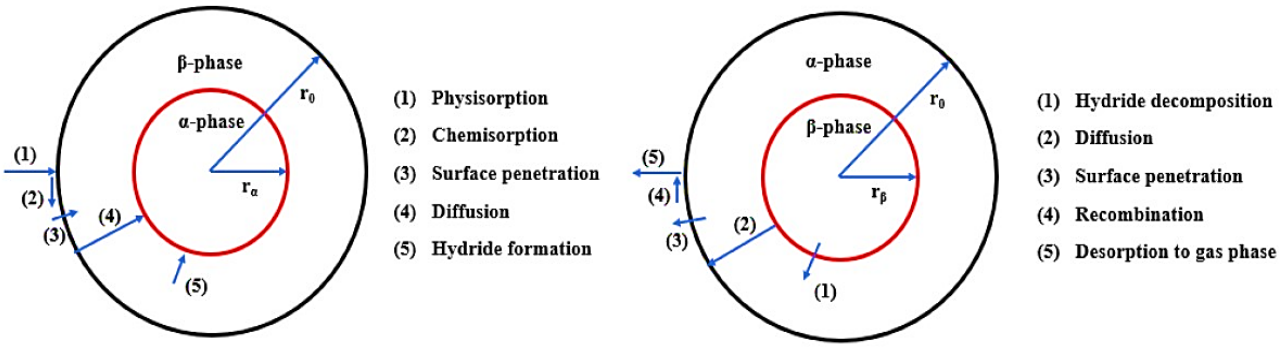

Fig. 16. Reaction steps of hydrogen adsorption (left) and desorption (right) by a spherical particle of metal/hydride powder [124].

Recombination into hydrogen molecules, surface penetration, diffusion of hydrogen atoms, hydride breakdown, and desorption into the gas phase are the steps involved in hydrogen absorption. A rate-limiting phase must also be included in hydrogen absorption to be managed while other actions are completed in balance. However, there are differences between the rate control mechanisms used in dehydrogenation and hydrogenation. Physical adsorption is typically not regarded as a limiting step because it requires relatively little activation energy to adsorb an H_2 molecule on a metal surface. There may be speed limits on the remaining steps. For dehydrogenation, steps 1, 2, and 3 (shown in Fig. 16) can be considered as possible rate-limiting steps [5].

The final stage of magnesium hydrogenation can be thought of as the nucleation and development of the MgH_2 phase. Because magnesium metal and its constituent hydride have different crystal structures, the nucleation and development of the hydride phase result in notable surface energy shifts [125].

Pure magnesium and MgH_2 in a coarse powder state show slow kinetics for hydrogen absorption and release, which usually low rate of hydrogenation of magnesium, as well as the rate of hydrogen in the matrix (field) are some of the intrinsic elements that require a temperature of more than 400 °C for the reaction. The determine the speed increase [5]. The rate-limiting step in dehydrogenation of MgH_2, can be increased by adding and doping several substances. The dissociation of hydrogen molecules, the diffusion of hydrogen through the surface, and the diffusion magnesium hydrogenation is thought to be the dissociation of hydrogen molecules on the magnesium surface. The energy needed for the hydrogen molecules on magnesium surfaces to dissociate is displayed in Table 4. Magnesium surfaces have been reported to have hydrogen dissociation energies between 0.4 and 1.1515 eV, which is higher than that of the majority of transition metals, including Ti, VNi, and Fe [126]. This indicates that on pure magnesium (0001) surfaces, a significant amount of energy must be overcome to dissociate H_2 [127]. Another inherent problem is the low rate of hydrogen diffusion in MgH_2.

Table 4. Dissociation energy of hydrogen molecule on Mg surface [127].

Metal	Metal dissociation energy (eV)
Pure Mg	Pure Mg 0.87–1.00
Ti-doped Mg	Null, negligible
Ni-doped Mg	0.06
V-doped Mg	Null
Cu-doped Mg	0.56
Pd-doped Mg	0.39
Fe-doped Mg	0.03
Ag-doped Mg	1.18

Table 4 shows the geometric model of the reaction of an Mg/MgH_2 particle based on the model of the hydride layer that forms on the particle's surface during hydrogenation. In addition, hydrogen atoms diffuse in the hydride phase at a far slower pace than in the metal phase. The hydrogen (DH) diffusion coefficient in MgH_2 is extremely low, Spatz et al. [128].

Alloying MgH_2/Mg is one of the best ways to lower its thermodynamic barrier. The creation of magnesium alloys alters the absorption path of MgH_2 rather than causing a direct interaction between Mg and Mg. The operating temperature of MgH_2/Mg can also be lowered by creating more thermodynamically stable alloys [129]. Table 5 presents the fundamental characteristics of a few hydrogen storage alloys based on magnesium.

According to Kumar et al., the Mg_2NiH_4 nanocrystalline alloy begins to absorb hydrogen at 200 °C. Nevertheless, the hydrogen capacity of Mg_2NiH_4 alloys was just 3.6% by weight. In the meantime, Mg_2FeH_6 exhibits an even greater enthalpy of 95 $kJ.mol^{-1}$ H_2, despite having a higher theoretical hydrogen capacity of 5.5 weight percent [135]. According to Chen et al., $Mg_2FeH_6@MgH_2$ demonstrated hydrogen storage capabilities, releasing 5% of its weight in hydrogen over 50 minutes at 280 °C [136].

Table 5. Basic information of some magnesium base alloys [130].

Name	E_a (kJ.mol^{-1})	ΔH (kJ.mol^{-1} H_2)	Capacity (wt%)	T (°C)	Ref.
Mg	-	74.5	7.6	300	[3]
Mg (2–8 nm)	-	74.2	7.6	273	[2]
$Mg_{90}Ce_{10}Ni_{10}$	109.2	77.9	5.4	284	[131]
Mg_2Ni	-	64.5	3.6	254	[18]
$Mg_3LaNi_{0.1}$	-	81	2.73	284	[132]
Mg_3Cd	69	65.5	2.8	-	[133]
Mg_3Ag	-	68.2	2.1	-	[134]

The addition of heavy metals lowers the system's ability to absorb hydrogen, while magnesium-based hydrogen storage alloys can generally lower the reaction temperature. Zhou et al. [5] stated that a one to five percent addition of TM catalyst resulted in a significant improvement, while the hydrogen storage capacity did not decrease. Table 6 summarizes the reported results of MgH_2 systems with Ti-based additives, as well as the synthesis method, pressure, temperature, weight percentage, and reaction time for adsorption and desorption processes. The findings demonstrate that Ti-based additions significantly improve MgH_2's capacity to store hydrogen.

8. Characterization and various analyses performed on magnesium hydride

8.1. SEM & TEM analysis

The absorption of hydrogen in magnesium was investigated by Vigeholm et al. [149] at temperatures between 260 and 425 °C and pressures equal to 2 MPa. At constant temperature, they concluded that the rate of absorption depends on the pressure, while the total absorption is achieved almost at the same time, regardless of the pressure.

Table 6. Magnesium's hydrogen storage capabilities with various Ti-based catalysts.

Material	Synthesis method	Hydrogen storage properties		Ref.
		Desorption kinetics	Absorption kinetics	
Mg-2% Ti	Ball mill (argon gas)	4.50%- 320 °C-0.2 bar-25 min	4.8%-320 °C-8 bar-21 min	[137]
MgH_2-2 at% Ti	Ball mill	6.32%- 623 K-35 kPa-0.5 h	6.32%-632 K-2000 kPa-4 min	[138]
MgH_2-4 mol% Ti	Ball mill	1.10%- 573 K- 2 MPa- 5 min	6.40%-573 K-2 MPa-5 min	[139]
MgH_2-5 at% Ti	Ball mill	5.50%-523 K-0.015 MPa-20 min	4.20%-373 K-1.0 MPa-15 min	[140]
Mg-5% Ti	CVD	---	---	[141]
MgH_2-20% Ti	Ball mill	0.12% 573 K-1 bar- 60 min	3.48%-573 K-12 bar-60 min	[142]
MgH_2-coated Ti	Ball mill	5.00%- 250 °C-15 min	---	[143]
MgH_2 4 mol% TiH_2	Ball mill	0.70%-573 K-2 MPa-5 min	6.10%-573 K-2 MPa- 5 min	[139]
MgH_2 10 mol% TiH_2	Ball mill	---	5.70%-240 °C-2 MPa-200 s	[144]
MgH_2-10% TiO_2	Ball mill	6.00%-300 °C-vacuum-20 min	6.00%-300 °C-0.84 MPa-5 min	[145]
Mg-20% TiO_2	Ball mill reactive	4.40%-350 °C-1 bar-8.5 min	3.80%-350 °C-20 bar-2 min	[146]
MgH_2 4 mol% TiF_3	Ball mill	4.50%-573 °C-2 MPa-5 min	5.10%-573 K-2 MPa-5 min	[139]
MgH_2 4 mol% $TiCl_3$	Ball mill	3.70%-583 K-2 MPa-5 min	5.30%-573 K-2 MPa-5 min	[139]
MgH_2 5 at% TiAl	Ball mill	4.90%-270 °C-0.12 bar-10 min	2.50%-25 °C-1 bar-250 min	[140]
MgH_2 5 at% TiNb	Ball mill	5.90%-27 °C-0.12 bar-10 min	2.80%-25 °C-1 bar-250 min	[147]
MgH_2-5% FeTi	Ball mill	---	2.30%-150 °C-2 MPa-5 min	[148]
MgH_2-5 at% $TiMn_2$	Ball mill	4.80%-270 °C-0.12 bar-10 min	3.20%-25 °C-1 bar-250 min	[140]
MgH_2-5 at% TiVMn	Ball mill	5.70%-270 °C-0.12 bar-10 min	3.00%-25 °C-1 bar-250 min	[140]

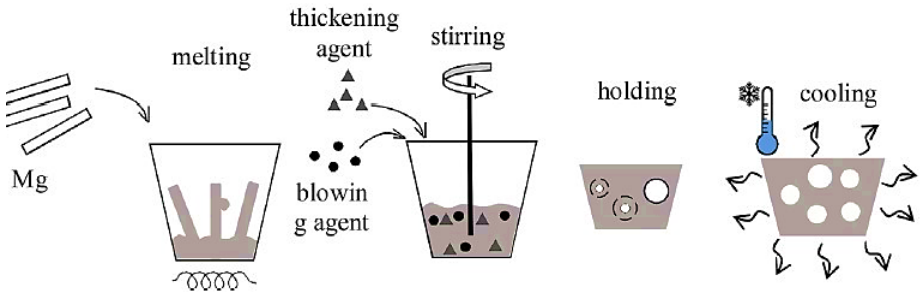

Fig. 17. Schematic image of the melt foaming process [150].

Hout et al. [85] found that each particle was a solid block of MgH_2 with a smooth surface before grinding and that the particles grew smaller following grinding in their investigation on the structural and kinetic examination of magnesium hydride hydrogen absorption utilizing the high-energy ball mill technique. The bigger particles in the ball-milled powder were aggregates of many smaller particles, and they had several elevations and depressions on their surface.

Hanada et al.'s study examined the connection between crystallographic characteristics and hydrogen storage in nanostructured magnesium hydride (MgH_2) that was made by mechanically milling it in an environment of hydrogen gas. MgH_2 nanostructures were created in this study by mechanically grinding them in a hydrogen gas atmosphere. During the first two hours of grinding, the amount of desorbed hydrogen was reduced by 16 weight percent, from 7.3 to 6.1% by weight [88].

In research by Bhatnagar et al. [69] on the synthesis of MgH_2 using the autocatalytic effect of MgH_2, they concluded that MgH_2 synthesized using 30 atm of H_2 pressure during ball milling followed by heat treatment and sintering, which was named $MgH_2$30BM, is the optimal material because it has the lowest desorption temperature (325 °C) and the highest weight percentage (6.60 wt%) of hydrogenation.

Kucharczyk et al. [150] discussed the characteristics, surface alterations, and manufacturing processes of porous structures composed of magnesium and its alloys. Controlling the temperature drop is essential for hydrogen solubility because liquid magnesium becomes supersaturated with hydrogen before solidification, forming bubbles. Using a concentration-cost-effective method that involves adding a blowing agent to the analyzer and evaporating it to create gas bubbles is one way to get around this. The quality of the final metal foam is influenced by the blowing agent's wetting and thermal stability (Fig. 17a).

Due to this method, magnesium is melted at a steady 720 °C in a crucible. Typically, a thickening agent such as calcium, SiC, or Al_2O_3 is added at a weight percentage of 2–5% to raise the viscosity. The magnesium alloy's ignition point is then raised to 800 °C by calcium. Additionally, to prevent magnesium fire, a CO_2 and SF_6 gas mixture is employed during the entire production process. A blowing agent is then used to swirl the liquid for approximately 30 seconds to spread it uniformly. At an atmospheric temperature of 825 °C, $CaCO_3$ is reported to break down into CO_2 and CaO. The likelihood of this reaction is low when compared to the temperature of molten magnesium. The foamy gas CO caused an exothermic reaction, according to a TGA-DTA investigation [151] conducted on the identical combination that had been heated above the melting temperature of magnesium. It was due to the decomposition of magnesium hydroxide.

A passive layer of SiO_2 can be applied on $CaCO_3$ particles to raise the reaction's initial temperature and enhance the blowing agent's thermal stability [152]. Using hydrochloric acid to stir, the $CaCO_3$ particles are combined with the $Na_2O.nSiO_2$ solution to create a slurry and keep the pH at around 12. A layer of SiO_2 forms on top of the $CaCO_3$ particles as a result of chemical reactions. Furthermore, the coating raises the temperature of the reaction between magnesium and the blowing agent by roughly 40 °C, improving a particle's thermal stability and giving the particles more time to disperse uniformly while stirring and allowing bubbles to gradually form at the bottom.

Melted magnesium is applied via the preform infiltration method to a porous substance, which is then removed once it has frozen (Fig. 18a). Therefore, the preform, which is a porous space-holding structure that is formed in separate phases, should have the following characteristics: appropriate particle arrangement, low reactivity with liquid magnesium, thermal resilience, and ease of washing to leave the desired pore configuration in the magnesium casting. The wetness of the preform also affects the quality of magnesium penetration. Insufficient wettability between liquid magnesium and solid preform (often NaCl) decreases the depth and rate of penetration of smaller holes [150]. Furthermore, fresh ossification development and cell infiltration are hindered by smooth pore walls. Rough surfaces and irregular pore walls are more favorable for cell infiltration and new ossification formation [153].

Higher pressures generally enable penetration into extremely small pores, roughening the pore walls, which is highly advantageous for cell growth within the pores. The porous structure of AZ91 infiltrated by the casting process at a pressure of 90 MPa is depicted in Fig. 18b–c. The metal frame profile shows higher stiffness and better energy absorption [153].

Typically having a granularity of 50 to 400 mm, common salt (sodium chloride) is one of the most readily available preform materials. To produce only grains of the necessary diameter that form equal-sized pores in the porous magnesium, the NaCl particles must first be sieved before usage. To create mechanically stable open porosity preforms, the particles undergo heat treatment. Additionally, it is feasible to generate the phenomenon of diffusion in grain boundaries and partial melting of salt to create a bottleneck between particles due to the high sintering temperature (785–750 °C), which is close to the melting point of salt (Fig. 18c). Low-density yet robust structures are produced as the sintering duration increases, particularly for finer grains. These constructions are

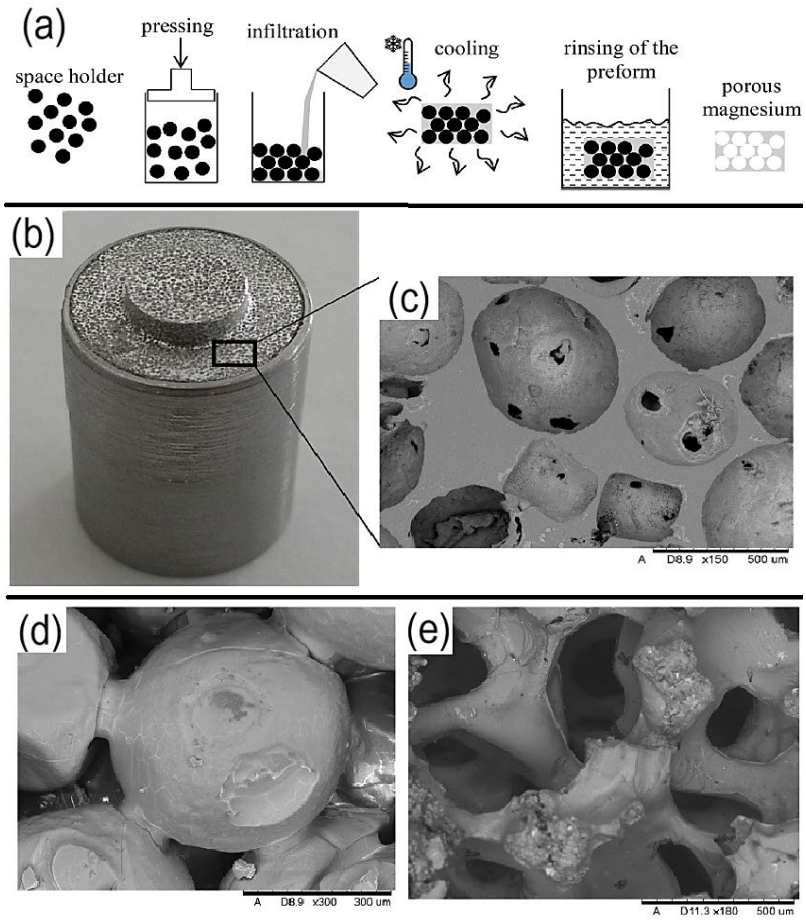

Fig. 18. The preform infiltration process is shown schematically in a) magnesium (AZ91) porous casting in a steel casing, which is the result of pressure casting infiltration of a salt preform; interconnected pores are seen after washing; the preform salt is sintered at 780 °C for 50 minutes; and the magnesium porous structure is created in the preform base at 780 °C for 22 hours [150].

frequently preferred in applications requiring strong, lightweight materials.

Also, these low-density structures are more stable during penetration and are easily washed away, resulting in a highly porous metal structure (Fig. 18d–e). Some techniques involve adding the sieved salt particles to a rubber mold, distributing them evenly, and then cold isostatically [154] pressing them to create a porous compact. In order to build a stable structure between the table salt grains after one to three hours, another way of performing production involves pouring the moistened grains into a core box and then dehumidifying them at 200 °C. The next step is to carefully remove the core box, leaving behind the stable salt performance [155].

When a rise in the sample's weight is noticed as a result of $Mg(OH)_2$ deposition, corrosion has begun. Additionally, because fluids may move more freely in wider gaps, weight loss occurs more quickly at higher porosity levels. Both the exterior and the interior of the pores of porous magnesium corrode [156]. Crucially, after seven days of submersion, porous magnesium maintains its porous structure, and its mechanical strength declines more gradually than that of bulk magnesium [157]. Studies for biomedical applications have generally found that magnesium corrodes quite quickly. Consequently, it is necessary to regulate the rusting process. [158]. However, studies have indicated that porous magnesium coated with hydroxyapatite has comparable characteristics to porous magnesium that is not coated [158–160].

Liu et al. conducted a study on the impact of air exposure on hydrogen storage capabilities utilizing magnesium hydride. Following a 15-minute exposure to air, a TEM investigation of the MgH_2-5% $TiMn_2$ structure was carried out. The MgH_2-5% $TiMn_2$ powder was dispersed in hexane to deposit hydride particles on the copper (Cu) network, as should be mentioned. Following dispersion, air drying was used to remove the hexane, and the sample was unavoidably exposed to ambient air for a few minutes before the TEM investigation. There is minimal particle-level contamination as a result of this technique [70].

8.2. TGA & DSC analysis

The dehydrogenation temperature of catalyzed magnesium hydride was considerably lower than that of other samples, according to Zhou et al.'s study on the thermodynamic and kinetic correlations of magnesium hydride. At around 100 °C, magnesium hydride began to lose weight (i.e., release hydrogen), which is too low a temperature to hydrogenate magnesium-based hydrides. All four samples'

dehydrogenation thermal analysis (TGA) curves are displayed in Fig. 19a.

Furthermore, TGA analysis was carried out at 120 and 150 °C, as Fig. 19b illustrates. This graph demonstrates that hydrogen can be slowly released from magnesium alloy hydride that has been catalyzed at 120 °C. The sample dehydrogenated considerably more quickly and completely in 3 hours when the TGA analysis was carried out at a temperature higher than 150 °C [161].

Additionally, Kudiyarov et al.'s DSC and thermogravimetric (TG) analyses of the magnesium hydride MgH_2-5 wt% SWCNT composite (at 300 rpm) are displayed in Fig. 20. According to the DSC results, magnesium hydride exhibits a large endothermic peak that is associated with the material's hydrogen emission. When heating magnesium hydride at a rate of 6 °C per minute, the maximum desorption temperature is 446 °C. A lower hydrogen desorption temperature of 420 °C is detected for the composition of MgH_2-5 weight percent SWCNT, which was produced by milling at 300 rpm. Thus, SWCNT can enhance magnesium hydride's hydrogen desorption capabilities [21].

A weight shift of 1.36% occurs at the start and finish of hydrogen desorption at a relatively low temperature, according to the TGA diagram. Tiny magnesium particles are present, which indicates this problem. These extremely small particles can be created via high-speed, high-energy milling and are distinguished by their greater hydrogen mobility [21].

8.3. FT-IR analysis

Qin et al. examined the morphological and structural features of MgH_2 materials doped with $LiBH_4$ to ascertain the state of the MgH_2 system doped with $LiBH_4$ following desorption and absorption. $LiBH_4$ peaks were not seen in the XRD patterns, except for the MgH_2/Mg phases, as shown in Fig. 21a. Interestingly, Fig. 21b of the FTIR results shows that the characteristic B-H vibrational bonds and $LiBH_4$ stretching bond are seen at the corresponding wavenumbers 2359, 2293, and 2225 cm^{-1}. Additionally, $LiBH_4$ does not break down or react to produce a new phase during decomposition; rather, it forms in amorphous and nanocrystalline states. As demonstrated by XPS analysis in Fig. 21c, $LiBH_4$ indicates the stable existence of $LiBH_4$ in cyclic $LiBH_4$-doped MgH_2. The binding energy shifts in the analysis provide additional evidence for the stable presence of $LiBH_4$ in cyclic $LiBH_4$-doped MgH_2 [4].

Furthermore, Fig. 21d–i shows the MgH_2 doped with $LiBH_4$'s morphological development and elemental distribution during the milling cycle. The morphology of particles with an average size of 1 to 2 μm is noticed before and after the cycle, as is the bonding phenomenon brought on by sintering after heating to absorb hydrogen. These findings demonstrate that $LiBH_4$'s fine distribution considerably prevents Mg grain development, which explains why the hydrogen adsorption and desorption peaks in Fig. 13 were obtained by these researchers.

Ultimately, the kinetic and stable cycling properties of hydrogen were much enhanced by these researchers' effective introduction of 5% by weight of $LiBH_4$ into the MgH_2 hydrogen storage system. Two crucial elements that prevent the formation of magnesium grains are necessary for the proper operation of an amorphous layer and uniform dispersion of $LiBH_4$. The evenly spaced $LiBH_4$ droplets in the MgH_2 matrix function as a quick hydrogen transfer during heating. The results of these studies point to a novel approach for boosting ionic hydrides' and other hydride systems' hydrogen absorption for hydrogen storage [4].

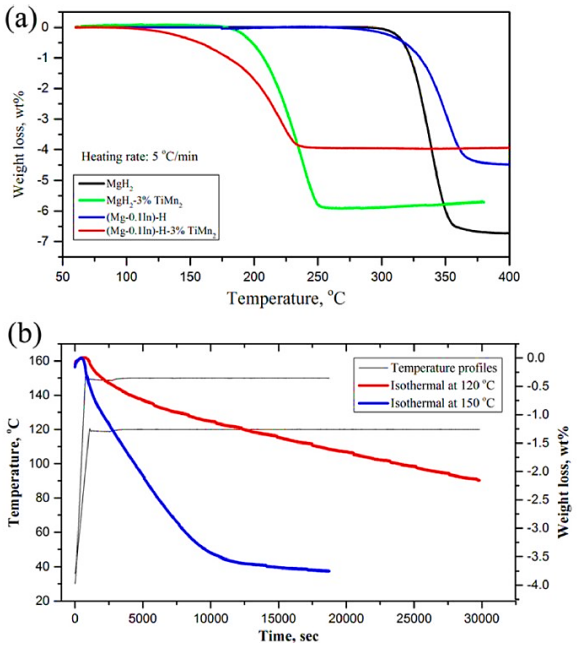

Fig. 19. Significant variations in the hydrogen desorption behavior were found when the TGA curves for a) MgH_2-0.1In doped by 3-atom $TiMn_2$ catalysts, MgH_2-0.1In, MgH_2 doped with 3-atom $TiMn_2$, and milled MgH_2 were compared with b) the $TiMn_2$ dehydrogenation curves of MgH_2-0.1 at 120 °C and 150 °C [161].

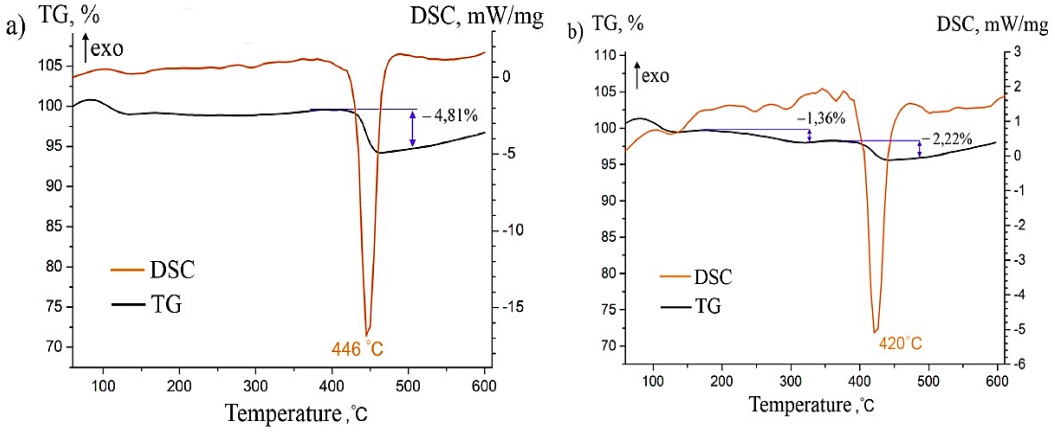

Fig. 20. a) Results of TG analysis for magnesium hydride and MgH_2-5 wt% SWCNT composite, and b) the results of analysis [21].

Researchers have so far worked hard to lower the temperature at which hydrogen adsorption and desorption occur and to speed up the adsorption/desorption mechanism; most of them were based on changing the microstructure by mechanical alloying or using a suitable catalyst (in elemental or composite form) [104].

Nevertheless, there are still obstacles in the way of developing effective hydrogen storage systems. The utilization of metal-organic frameworks (MOFs) as possible hydrogen storage materials is one promising strategy that has drawn interest recently. MOFs are a type of porous material with a large surface area and adjustable pore size for effective hydrogen adsorption. They are made up of metal ions or clusters connected by organic ligands [162].

9. Applications of materials based on MgH_2 for the hydrogen storage

The new energy structure, "renewable energy for hydrogen storage", was clearly envisioned for the future in this study (Fig. 22). In general,

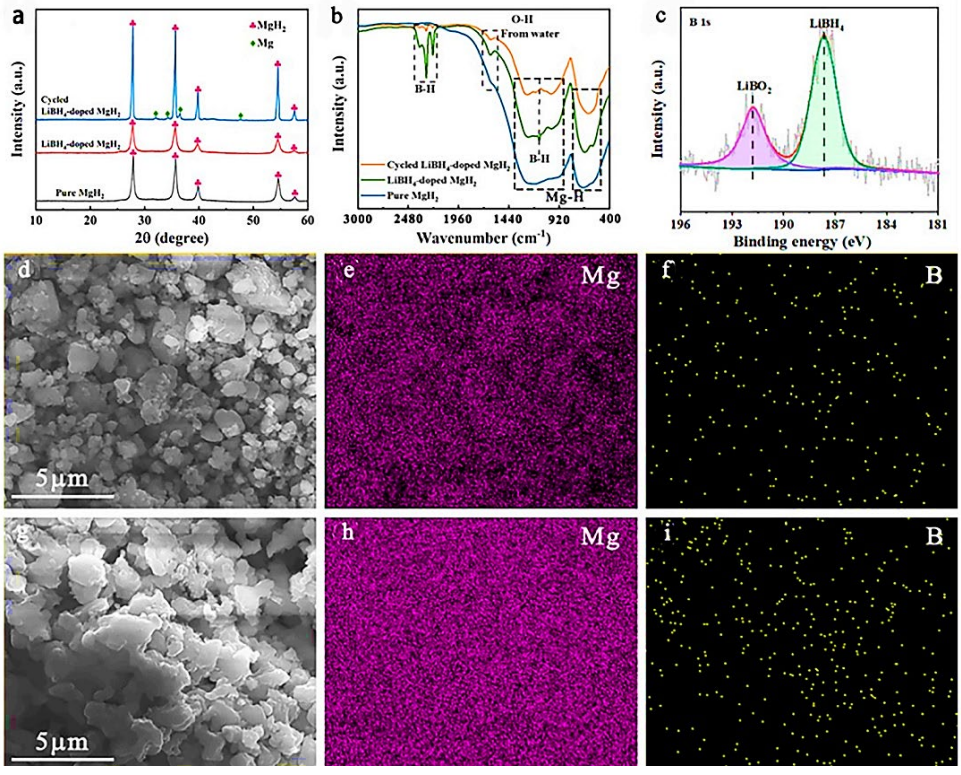

Fig. 21. a) XRD patterns, b) FTIR spectra, and c) XPS spectra of pure MgH_2 and $LiBH_4$-doped MgH_2 samples after milling and cycling. FESEM images of the $LiBH_4$-doped MgH_2 sample d) before and g) after cycling, with corresponding e, h) Mg element maps, and f, i) multi-element maps [4].

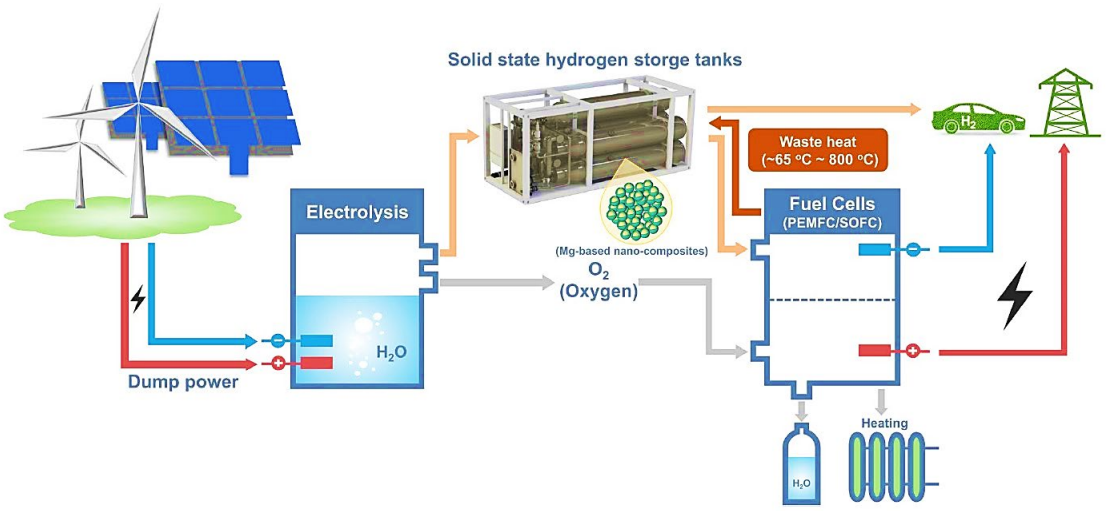

Fig. 22. Prospects of energy storage infrastructure in the future [6].

hydrogen can be produced and stored in magnesium-based hydrogen storage tanks by electrolyzing water using electricity derived from clean energy sources. This system can simultaneously supply high-purity hydrogen gas to a fuel cell for power generation or other industrial uses. Thus, the stored energy can be used to propel the constant release of hydrogen from hydrogen storage tanks [5].

MgH_2 exhibits encouraging possibilities for weight and volume capabilities when compared to $LaNi_5$-based materials and Ti-V(Cr)-based alloys with center-filled cubic structures. Furthermore, the hydrogen supply via the hydrolysis reaction in water is extremely promising for small-scale portable applications because of the cost and energy density of MgH_2. It is also important to note that the MgH_2 nanostructures enhance the hydrolysis reaction's performance and make it more practical and efficient for portable, small-scale applications [6].

Furthermore, MgH_2 can be utilized for large-scale energy storage in solar power plants or businesses due to its high storage density (3060 $kJ.kg^{-1}$), great reversibility, and low cost [22]. In the field of chemical heat storage, this is one of the most popular research areas. MgH_2 can be broken down throughout the day using excess solar energy, and hydrogen can be stored at low temperatures in a hydrogen tank or other hydrogen storage material. To increase the MgH_2/Mg system's heat storage efficiency, more catalysts ought to be added. Naturally, it should be noted that estimating the cost of this sector is challenging. The utilization of nanostructured magnesium-based hydrogen storage materials would result in significant cost savings for heat storage systems if the synthesis process for these materials can be established at the nanoscale.

According to this study, the synthesized material is anticipated to undergo one or more cycles of change in characteristics under normal hydrogenation or dehydrogenation circumstances of magnesium-based materials in dynamic systems. Grain growth and the release of significant species are the results of hydrogenation, which is carried out at a high temperature. This straightforward process of hydrogen entering and leaving the lattice can therefore alter the crystal structure. When creating novel materials and implementing them in their intended uses, this problem should be considered.

It has also been found that the kinetics of hydrogenation or dehydrogenation can be dramatically improved by using suitable catalysts. In terms of suitable hydrogen storage materials, it is associated with a large heat of reaction; to use these materials in real conditions, the great challenge will be to improve the heat transfer. Alloying magnesium with other metals can enhance the thermodynamic features of the Mg-H system, but generally speaking, a fundamental understanding of the impact of nanocrystalline, catalyst addition, and chemical alteration is necessary. However, mechanical changes of Mg/MgH_2 without additions show notable improvements due to the increase in storage capacity. It has been experimentally demonstrated that the nano-doping of magnesium improves the thermodynamic characteristics of Mg/MgH_2. Magnesium nanodoping has demonstrated encouraging outcomes in terms of increasing the hydrogen storage capacity.

The kinetics of hydrogen absorption and desorption in systems containing magnesium have also been shown to be enhanced by the addition of catalysts like titanium and nickel. These catalysts contribute to reducing the activation energy required for hydrogen uptake and release, making the process more efficient. Furthermore, chemical changes, such as the inclusion of carbon-based materials, have been shown to increase magnesium hydride stability and cycling performance. Overall, magnesium-based materials' capacity to store hydrogen might be greatly enhanced by chemical modification, catalyst addition, and nanocrystallinity.

The shift in entropy controls the notable decrease in reaction enthalpy observed in MgH_2-capped nanoparticles. Furthermore, these theoretical studies demonstrate that for very small clusters of magnesium atoms, a notable drop in the desorption energy may take place. According to the majority of researchers, every attempt to bring the size of the Mg/MgH_2 crystallite particles down to the nanoscale range improved the kinetics of the interaction with hydrogen. The primary concern, though, is maintaining the original nanostructure while cycling at high temperatures. During cycling, the use of nanoencapsulants may also aid in preventing grain sintering or recrystallization.

Reaction kinetics has definitely advanced significantly with the usage of additives. Even with the significant scientific efforts of the majority of researchers and the equipment at their disposal, a comprehensive explanation of the mechanism behind the catalytic actions of each additive is still lacking. For all additions, it is unknown if the action is

appropriately catalytic [78, 120, 161, 163–165]. Some additions have several uses and are not real catalysts because they aid in the breakdown, reduction, or formation of more complex compounds with magnesium after cycling. Additionally, creating more potent additives can be aided by knowing the mechanisms via which additives alter the kinetics of the Mg-H reaction.

10. Conclusions and outlook

Magnesium-based hydrides have demonstrated significant potential as thermal energy and hydrogen storage due to their high energy density. Mg-based materials are attractive because of their high hydrogen capacity, plentiful supplies, reversibility, and low toxicity. Ti doping-based addition is a well-known method of improving MgH_2's hydrogen storage capabilities. MgH_2 additive composites with nanomaterial structures are commonly created by combining ball milling processes with catalytic doping. Moreover, additional techniques have been employed, including chemical and thin-film deposition.

Several nanostructures can be produced from magnesium-based materials, and catalytic doping significantly increases their kinetics, according to a recent study. Hydrogenation and hydrogenation kinetics were improved by a variety of Ti-based catalyst types, including hydrides, oxides, halides, and intermetallics. An analysis of the reported activation energies reveals that Ti-based additions can significantly lower the energy barrier. Diffusion, development of the hydride nucleus, surface penetration, and hydrogen dissociation are the general phases that make up the catalytic mechanism for hydrogenation.

Although the exact function of Ti-based catalysts is yet unknown, there is proof that catalysts are crucial to the development of various processes. The doped catalyst species, according to the researchers, may lower the hydrogen molecule's dissociation energy barrier and promote hydrogen diffusion in the Mg/MgH_2 matrix. Another helpful tool for interpreting the reaction control processes is kinetic modeling. In order to give more precise comparisons with boundary conditions for various models utilized for interpretations, future mechanisms should also be focused on observing catalytic activity and microstructure evolution under extremely regulated reaction circumstances.

Porous nanomagnesium is becoming more and more popular, which indicates that researchers are interested in it. Numerous uses are made possible by the characteristics of the material that is produced. The need for sophisticated, biodegradable, and biocompatible materials has made biomedical applications the most attractive area of research. The use of foam in the building of floating things is demonstrated by its great mechanical strength and lower density than water. Their advantageous strength-to-density ratio helps laboratory centrifuge rotors reach faster speeds in addition to boosting vehicle speed and reducing fuel consumption. This study demonstrates the typical processes for creating porous nanoparticles based on magnesium, including their synthesis and manufacturing.

Additionally, magnesium's mechanical characteristics, corrosion resistance, and surface alterations have demonstrated that one of the primary challenges in the design of porous magnesium materials is striking a balance between porosity and mechanical resistance. It appears that designing the pore architecture in some way to produce comparatively smooth pore walls is a good method for a variety of applications. Thus, manufacturing techniques for isotropic porous magnesium with a strong focus on hydrogen storage applications should be part of future studies. Additionally, a better, easier, and more affordable production process needs to be developed. It is easier to automate a simpler procedure. The impact of porosity on the rate of corrosion of porous magnesium is widely recognized, although much more research is still required.

In general, in this research, magnesium hydride was milled with various analyses and characterizations, such as SEM, FE-SEM, FT-IR, TGA, DSC, XPS, and XRD. Using the obtained results, it is now possible to produce porous MgH_2 nanostructures with high precision. Also, after the ball mill is obtained, the distribution and checking of the properties of the sample should be performed. It was found that the high-energy part of the vibration spectra is relatively sensitive to the stresses caused by the ball mill. Certain phases whose spectra show a strong voltage dependence may be inelastic in the high-energy (i.e., above 50 mV) part of the spectrum. Ultimately, we deduce that the kinetics of hydrogen adsorption and desorption improved mostly due to particle size reduction, nanostructure, and encapsulation, rather than stresses and defects. It is also predicted that the same improvement in prepared and porous magnesium samples will have better performance and a high yield of hydrogen storage with other methods.

CRediT authorship contribution statement

Ali Borchloo: Conceptualization, Investigation, Writing – original draft, Writing – review & editing.

Khanali Nekoee: Project administration, Funding acquisition, Conceptualization, Writing – review & editing, Visualization, resources, Data curation.

Data availability

The data underlying this article will be shared on reasonable request to the corresponding author.

Declaration of competing interest

The authors declare no competing interests.

Funding and acknowledgment

This research did not receive any specific grant from funding agencies in the public, commercial, or not-for-profit sectors.

References

[1] I.P. Jain, C. Lal, A. Jain, Hydrogen storage in Mg: a most promising material, Int. J. Hydrog. Energy. 35 (2010) 5133–5144. https://doi.org/10.1016/j.ijhydene.2009.08.088.

[2] M. Paskevicius, D.A. Sheppard, C.E. Buckley, Thermodynamic changes in mechanochemically synthesized magnesium hydride nanoparticles, J. Am. Chem. Soc. 132 (2010) 5077–5083. https://doi.org/10.1021/ja908398u.

[3] J.F. Stampfer Jr, C. Holley Jr, J. Suttle, The magnesium-hydrogen system1-3, J. Am. Chem. Soc. 82 (1960) 3504–3508. https://doi.org/10.1021/ja01499a006.

[4] Z.-K. Qin, L.-Q. He, X.-L. Ding, T.-Z. Si, P. Cui, H.-W. Li, Y.-T. Li, Liquid Channels Built-In Solid Magnesium Hydrides for Boosting Hydrogen Sorption, Inorganics. 11 (2023) 216. https://doi.org/10.3390/inorganics11050216.

[5] C. Zhou, J. Zhang, R.C. Bowman, Z.Z. Fang, Roles of Ti-Based Catalysts on Magnesium Hydride and Its Hydrogen Storage Properties, Inorganics. 9 (2021) 36. https://doi.org/10.3390/inorganics9050036.
[6] L. Ren, Y. Li, N. Zhang, Z. Li, X. Lin, W. Zhu, C. Lu, W. Ding, J. Zou, Nanostructuring of Mg-Based Hydrogen Storage Materials: Recent Advances for Promoting Key Applications, Nano-micro Lett. 15 (2023) 93. https://doi.org/10.1007/s40820-023-01041-5.
[7] M. Lutz, M. Linder, I. Bürger, High capacity, low pressure hydrogen storage based on magnesium hydride and thermochemical heat storage: Experimental proof of concept, Appl. Energy. 271 (2020) 115226. https://doi.org/10.1016/j.apenergy.2020.115226.
[8] J.C. Crivello, B. Dam, R.V. Denys, M. Dornheim, D.M. Grant, et al., Review of magnesium hydride-based materials: development and optimisation, Appl. Phys. A. 122 (2016) 97. https://doi.org/10.1007/s00339-016-9602-0.
[9] J. Huot, D.B. Ravnsbæk, J. Zhang, F. Cuevas, M. Latroche, T.R. Jensen, Mechanochemical synthesis of hydrogen storage materials, Prog. Mater. Sci. 58 (2013) 30–75. https://doi.org/10.1016/j.pmatsci.2012.07.001.
[10] P. Vajeeston, P. Ravindran, B. Hauback, H. Fjellvåg, A. Kjekshus, et al., Structural stability and pressure-induced phase transitions in MgH2, Phys. Rev. B - Condens. Matter Mater. Phys. 73 (2006) 224102. https://doi.org/10.1103/PhysRevB.73.224102.
[11] P. Marty, P. de Rango, B. Delhomme, S. Garrier, Various tools for optimizing large scale magnesium hydride storage, J. Alloys Compd. 580 (2013) S324-S328. https://doi.org/10.1016/j.jallcom.2013.02.169.
[12] W. Zachariasen, C. Holley, J. Stamper, Neutron diffraction study of magnesium deuteride, Acta Crystal. 16 (1963) 352–353. https://doi.org/10.1107/S0365110X63000967.
[13] M. Bortz, B. Bertheville, G. Böttger, K. Yvon, Structure of the high pressure phase γ-MgH2 by neutron powder diffraction, J. Alloys Compd. 287 (1999) L4–L6. https://doi.org/10.1016/S0925-8388(99)00028-6.
[14] J. Zheng, L. Chen, J. Wang, X. Xi, H. Zhu, Y. Zhou, J. Wang, Thermodynamic analysis and comparison of four insulation schemes for liquid hydrogen storage tank, Energy Convers. Manage. 186 (2019) 526–534. https://doi.org/10.1016/j.enconman.2019.02.073.
[15] Z. Chen, K.O. Kirlikovali, K.B. Idrees, M.C. Wasson, O.K. Farha, Porous materials for hydrogen storage, Chem. 8 (2022) 693–716. https://doi.org/10.1016/j.chempr.2022.01.012.
[16] L. Ouyang, K. Chen, J. Jiang, X.-S. Yang, M. Zhu, Hydrogen storage in light-metal based systems: A review, J. Alloys Compd. 829 (2020) 154597. https://doi.org/10.1016/j.jallcom.2020.154597.
[17] B. Sakintuna, F. Lamari-Darkrim, M. Hirscher, Metal hydride materials for solid hydrogen storage: a review, Int. J. Hydrog. Energy. 32 (2007) 1121–1140. https://doi.org/10.1016/j.ijhydene.2006.11.022.
[18] J.J. Reilly Jr, R.H. Wiswall Jr, Reaction of hydrogen with alloys of magnesium and nickel and the formation of Mg2NiH4, Inorg. Chem. 7 (1968) 2254–2256. https://doi.org/10.1021/ic50069a016.
[19] S. Halilov, D. Singh, M. Gupta, R. Gupta, Stability and electronic structure of the complex K 2 Pt Cl 6-structure hydrides DMH 6 (D= Mg, Ca, Sr; M= Fe, Ru, Os), Phys. Rev. B - Condens. Matter Mater. Phys. 70 (2004) 195117. https://doi.org/10.1103/PhysRevB.70.195117.
[20] X. Huang, X. Xiao, Y. He, Z. Yao, X. Ye, H. Kou, C. Chen, T. Huang, X. Fan, L. Chen, Probing an intermediate state by X-ray absorption near-edge structure in nickel-doped 2LiBH4–MgH2 reactive hydride composite at moderate temperature, Mater. Today Nano. 12 (2020) 100090. https://doi.org/10.1016/j.mtnano.2020.100090.
[21] V.N. Kudiyarov, R.R. Elman, N.E. Kurdyumov, The Effect of High-Energy Ball Milling Conditions on Microstructure and Hydrogen Desorption Properties of Magnesium Hydride and Single-Walled Carbon Nanotubes, Metals. 11 (2021) 1409. https://doi.org/10.3390/met11091409.
[22] D.S. Korablov, O.V. Bezdorozhev, S. Gierlotka, V.A. Yartys, Y.M. Solonin, Effect of Various Additives on the Hydrolysis Performance of Nanostructured MgH2 Synthesized by High-Energy Ball Milling in Hydrogen, Powder Metall. Met. Ceram. 59 (2021) 483–490. https://doi.org/10.1007/s11106-021-00193-6.
[23] G. Liang, J. Huot, S. Boily, A. Van Neste, R. Schulz, Hydrogen storage properties of the mechanically milled MgH2–V nanocomposite, J. Alloys Compd. 291 (1999) 295–299. https://doi.org/10.1016/S0925-8388(99)00268-6.
[24] F. Cuevas, D. Korablov, M. Latroche, Synthesis, structural and hydrogenation properties of Mg-rich MgH2–TiH2 nanocomposites prepared by reactive ball milling under hydrogen gas, Phys. Chem. Chem. Phys. 14 (2012) 1200–1211. https://doi.org/10.1039/C1CP23030A.
[25] D. Aurbach, R. Turgeman, O. Chusid, Y. Gofer, Spectroelectrochemical studies of magnesium deposition by in situ FTIR spectroscopy, Electrochem. Commun. 3 (2001) 252–261. https://doi.org/10.1016/S1388-2481(01)00148-5.
[26] T. Liu, C. Chen, H. Wang, Y. Wu, Enhanced Hydrogen Storage Properties of Mg–Ti–V Nanocomposite at Moderate Temperatures, J. Phys. Chem. C. 118 (2014) 22419–22425. https://doi.org/10.1021/jp5061073.
[27] A. Zaluska, L. Zaluski, J. Ström–Olsen, Nanocrystalline magnesium for hydrogen storage, J. Alloys Compd. 288 (1999) 217–225. https://doi.org/10.1016/S0925-8388(99)00073-0.
[28] G. Barkhordarian, T. Klassen, R. Bormann, Effect of Nb2O5 content on hydrogen reaction kinetics of Mg, J. Alloys Compd. 364 (2004) 242–246. https://doi.org/10.1016/S0925-8388(03)00530-9.
[29] B.S. Amirkhiz, B. Zahiri, P. Kalisvaart, D. Mitlin, Synergy of elemental Fe and Ti promoting low temperature hydrogen sorption cycling of magnesium, Int. J. Hydrog. Energy. 36 (2011) 6711–6722. https://doi.org/10.1016/j.ijhydene.2011.02.141.
[30] A. Pan, T. Kar, A.K. Rakshit, S.P. Moulik, Enthalpy-Entropy Compensation (EEC) Effect: Decisive Role of Free Energy, J. Phys. Chem. B. 120 (2016) 10531–10539. https://doi.org/10.1021/acs.jpcb.6b05890.
[31] A. Pan, T. Biswas, A.K. Rakshit, S.P. Moulik, Enthalpy-Entropy Compensation (EEC) Effect: A Revisit, J. Phys. Chem. B. 119 (2015) 15876–15884. https://doi.org/10.1021/acs.jpcb.5b09925.
[32] N. Patelli, M. Calizzi, L. Pasquini, Interface Enthalpy-Entropy Competition in Nanoscale Metal Hydrides, Inorganics. 6 (2018) 13. https://doi.org/10.3390/inorganics6010013.
[33] V. Berube, G. Chen, M. Dresselhaus, Impact of nanostructuring on the enthalpy of formation of metal hydrides, Int. J. Hydrog. Energy. 33 (2008) 4122–4131. https://doi.org/10.1016/j.ijhydene.2008.05.083.
[34] C. Zlotea, Y. Oumellal, S.-J. Hwang, C.M. Ghimbeu, P.E. de Jongh, M. Latroche, Ultrasmall MgH2 Nanoparticles Embedded in an Ordered Microporous Carbon Exhibiting Rapid Hydrogen Sorption Kinetics, J. Phys. Chem. C. 119 (2015) 18091–18098. https://doi.org/10.1021/acs.jpcc.5b05754.
[35] M. Konarova, A. Tanksale, J. Norberto Beltramini, G. Qing Lu, Effects of nano-confinement on the hydrogen desorption properties of MgH2, Nano Energy. 2 (2013) 98–104. https://doi.org/10.1016/j.nanoen.2012.07.024.
[36] L.K. Wagner, E.H. Majzoub, M.D. Allendorf, J.C. Grossman, Tuning metal hydride thermodynamics via size and composition: Li-H, Mg-H, Al-H, and Mg-Al-H nanoclusters for hydrogen storage, Phys. Chem. Chem. Phys. 14 (2012) 6611–6616. https://doi.org/10.1039/c2cp24063g.
[37] J. Huang, J.F. Wan, C. Xie, J. Chen, C. Long, Structure analysis of surface layer on passivated magnesium powders, Mater. Lett. 61 (2007) 2430–2433. https://doi.org/10.1016/j.matlet.2006.09.029.

[38] J. Boulet, N. Gerard, The mechanism and kinetics of hydride formation in Mg-10wt.% Ni and CeMg12, J. Less-Common Met. 89 (1983) 151–161. https://doi.org/10.1016/0022-5088(83)90261-8.
[39]N. B. Arboleda Jr, H. Kasai, K. Nobuhara, W. A. Diño, H. Nakanishi, Dissociation and sticking of H2 on Mg (0001), Ti (0001) and La (0001) surfaces, J. Phys. Soc. Jpn. 73 (2004) 745–748. https://doi.org/10.1143/JPSJ.73.745.
[40] B. Hammer, J.K. Nørskov, Electronic factors determining the reactivity of metal surfaces, Surf. Sci. 343 (1995) 211–220. https://doi.org/10.1016/0039-6028(96)80007-0.
[41] M. Stioui, A. Grayevsky, A. Resnik, D. Shaltiel, N. Kaplan, Macroscopic and microscopic kinetics of hydrogen in magnesium-rich compounds, J. Less-Common Met. 123 (1986) 9–24. https://doi.org/10.1016/0022-5088(86)90110-4.
[42] J. Töpler, H. Buchner, H. Säufferer, K. Knorr, W. Prandl, Measurements of the diffusion of hydrogen atoms in magnesium and Mg2Ni by neutron scattering, J. Less-Common Met. 88 (1982) 397–404. https://doi.org/10.1016/0022-5088(82)90248-X.
[43] N.S. Norberg, T.S. Arthur, S.J. Fredrick, A.L. Prieto, Size-dependent hydrogen storage properties of Mg nanocrystals prepared from solution, J. Am. Chem. Soc. 133 (2011) 10679–10681. https://doi.org/10.1021/ja201791y.
[44] Y. Sun, C. Shen, Q. Lai, W. Liu, D.-W. Wang, K.-F. Aguey-Zinsou, Tailoring magnesium based materials for hydrogen storage through synthesis: Current state of the art, Energy Storage Mater. 10 (2018) 168–198. https://doi.org/10.1016/j.ensm.2017.01.010.
[45] R. Schulz, J. Huot, G. Liang, S. Boily, G. Lalande, M. Denis, J. Dodelet, Recent developments in the applications of nanocrystalline materials to hydrogen technologies, Mater. Sci. Eng: A. 267 (1999) 240–245. https://doi.org/10.1016/S0921-5093(99)00098-2.
[46]Y. Fu, L. Zhang, Y. Li, S. Guo, Z. Yu, W. Wang, K. Ren, Q. Peng, S. Han, Catalytic effect of MOF-derived transition metal catalyst FeCoS@ C on hydrogen storage of magnesium, J. Mater. Sci. Technol. 138 (2023) 59–69. https://doi.org/10.1016/j.jmst.2022.08.019.
[47] M. Felderhoff, B. Bogdanović, High temperature metal hydrides as heat storage materials for solar and related applications, Int. J. Mol. Sci. 10 (2009) 325–344. https://doi.org/10.3390/ijms10010325.
[48] P.E. de Jongh, P. Adelhelm, Nanosizing and nanoconfinement: new strategies towards meeting hydrogen storage goals, ChemSusChem. 3 (2010) 1332–1348. https://doi.org/10.1002/cssc.201000248.
[49] R.W. Wagemans, J.H. van Lenthe, P.E. de Jongh, A.J. van Dillen, K.P. de Jong, Hydrogen storage in magnesium clusters: quantum chemical study, J. Am. Chem. Soc. 127 (2005) 16675–16680. https://doi.org/10.1021/ja054569h.
[50] S. Krieck, H. Görls, M. Westerhausen, Mechanistic elucidation of the formation of the inverse Ca (I) sandwich complex [(thf) 3Ca (μ-C6H3-1, 3, 5-Ph3) Ca (thf) 3] and stability of aryl-substituted phenylcalcium complexes, J. Am. Chem. Soc. 132 (2010) 12492–12501. https://doi.org/10.1021/ja105534w.
[51] S.J. Bonyhady, D. Collis, G. Frenking, N. Holzmann, C. Jones, A. Stasch, Synthesis of a stable adduct of dialane(4) (Al2H4) via hydrogenation of a magnesium(I) dimer, Nat. Chem. 2 (2010) 865–869. https://doi.org/10.1038/nchem.762.
[52] J. Intemann, J. Spielmann, P. Sirsch, S. Harder, Well-defined molecular magnesium hydride clusters: relationship between size and hydrogen-elimination temperature, Chemistry. 19 (2013) 8478–8489. https://doi.org/10.1002/chem.201300684.
[53] A. Pan, B. Mandal, A.K. Rakshit, S.P. Moulik, A Rational Study of the Origin and Generality of Anti-Enthalpy–Entropy Compensation (AEEC) Phenomenon, Z. Phys. Chem. 232 (2018) 373–391. https://doi.org/10.1515/zpch-2017-1007.
[54] Y. Wang, Y. Wang, Recent advances in additive-enhanced magnesium hydride for hydrogen storage, Prog. Nat. Sci: Mater. Int. 27 (2017) 41–49. https://doi.org/10.1016/j.pnsc.2016.12.016.
[55] Q. Hou, X. Yang, J. Zhang, Review on hydrogen storage performance of MgH2: development and trends, ChemistrySelect. 6 (2021) 1589–1606. https://doi.org/10.1002/slct.202004476.
[56] W. Liu, K.-F. Aguey-Zinsou, Synthesis of highly dispersed nanosized LaNi5 on carbon: Revisiting particle size effects on hydrogen storage properties, Int. J. Hydrog. Energy. 41 (2016) 14429–14436. https://doi.org/10.1016/j.ijhydene.2016.02.024.
[57] E. Wiberg, H. Goeltzer, R. Bauer, Synthese von Magnesiumhydrid aus den Elementen, Z. Naturforsch. - B. 6 (1951) 394–395. https://doi.org/10.1515/znb-1951-0714.
[58] X. Wang, L. Andrews, Infrared spectra of magnesium hydride molecules, complexes, and solid magnesium dihydride, J. Phys. Chem. A. 108 (2004) 11511–11520. https://doi.org/10.1021/jp046410h.
[59] P. Vajeeston, P. Ravindran, A. Kjekshus, H. Fjellvag, Pressure-induced structural transitions in MgH2, Phys Rev Lett. 89 (2002) 175506. https://doi.org/10.1103/PhysRevLett.89.175506.
[60] D. Mukherjee, J. Okuda, Molecular Magnesium Hydrides, Angew. Chem. Int. Ed. Engl. 57 (2018) 1458–1473. https://doi.org/10.1002/anie.201708592.
[61] D. Gallagher, K. Henderson, A. Kennedy, C.T. O' Hara, R.E. Mulvey, R.B. Rowlings, Chem. Commun. 2002 (2002) 376–377. http://dx.doi.org/10.1039/b110117j.
[62] H. Leng, Y. Pan, Q. Li, K.C. Chou, Effect of LiH on hydrogen storage property of MgH2, Int. J. Hydrog. Energy. 39 (2014) 13622–13627. https://doi.org/10.1016/j.ijhydene.2014.02.131.
[63] S.-I. Ri, K.-J. Um, J.-H. Wi, J.-C. Kim, N.-H. Kim, Effects of single– and co– substitution of Ti and Fe on vacancy formation and dehydrogenation from MgH2 (110) surface: Ab initio study, Int. J. Hydrog. Energy. 44 (2019) 22761–22769. https://doi.org/10.1016/j.ijhydene.2019.06.213.
[64] A. Borgschulte, U. Bösenberg, G. Barkhordarian, M. Dornheim, R. Bormann, Enhanced hydrogen sorption kinetics of magnesium by destabilized MgH2− δ, Catal. Today. 120 (2007) 262–269. https://doi.org/10.1016/j.cattod.2006.09.031.
[65] M.H. Mintz, Y. Zeiri, Hydriding kinetics of powders, J. Alloys Compd. 216 (1995) 159–175. https://doi.org/10.1016/0925-8388(94)01269-N.
[66] G. Barkhordarian, T. Klassen, R. Bormann, Kinetic investigation of the effect of milling time on the hydrogen sorption reaction of magnesium catalyzed with different Nb2O5 contents, J. Alloys Compd. 407 (2006) 249–255. https://doi.org/10.1016/j.jallcom.2005.05.037.
[67] E. Evard, I. Gabis, V. Yartys, Kinetics of hydrogen evolution from MgH2: experimental studies, mechanism and modelling, Int. J. Hydrog. Energy. 35 (2010) 9060–9069. https://doi.org/10.1016/j.ijhydene.2010.05.092.
[68] M. Tegel, S. Schöne, B. Kieback , L. Röntzsch, An efficient hydrolysis of MgH2-based materials, Int. J. Hydrog. Energy. 42 (2017) 2167–2176. https://doi.org/10.1016/j.ijhydene.2016.09.084.
[69] A. Bhatnagar, M.A. Shaz, O.N. Srivastava, Synthesis of MgH2 using autocatalytic effect of MgH2, Int. J. Hydrog. Energy. 44 (2019) 6738–6747. https://doi.org/10.1016/j.ijhydene.2019.01.163.
[70] H. Liu, P. Sun, R.C. Bowman, Z.Z. Fang, Y. Liu, C. Zhou, Effect of air exposure on hydrogen storage properties of catalyzed magnesium hydride, J. Power Sources. 454 (2020) 227936. https://doi.org/10.1016/j.jpowsour.2020.227936.
[71] M. Polanski, J. Bystrzycki, T. Plocinski, The effect of milling conditions on microstructure and hydrogen absorption/desorption properties of magnesium hydride (MgH2) without and with Cr2O3 nanoparticles, Int. J. Hydrog. Energy. 33 (2008) 1859–1867. https://doi.org/10.1016/j.ijhydene.2008.01.043.
[72] T. He, H. Cao, P. Chen, Complex Hydrides for Energy Storage, Conversion, and Utilization, Adv. Mater. 31 (2019) e1902757. https://doi.org/10.1002/adma.201902757.
[73] V.A. Yartys, M.V. Lototskyy, E. Akiba, R. Albert, V.E. Antonov, et al., Magnesium based materials for hydrogen based energy storage:

Past, present and future, Int. J. Hydrog. Energy. 44 (2019) 7809–7859. https://doi.org/10.1016/j.ijhydene.2018.12.212.
[74] D. Elanski, J.-W. Lim, K. Mimura, M. Isshiki, Thermodynamic estimation of hydride formation during hydrogen plasma arc melting, J. Alloys Compd. 439 (2007) 210–214. https://doi.org/10.1016/j.jallcom.2006.04.076.
[75] J. Benjamin, T. Volin, The mechanism of mechanical alloying, Metall. Trans. 5 (1974) 1929–1934. https://doi.org/10.1007/bf02644161.
[76] C. Suryanarayana, Mechanical alloying and milling, Prog. Mater. Sci. 46 (2001) 1–184. https://doi.org/10.1016/S0079-6425(99)00010-9.
[77] S.-H. Hong, H.-J. Kim, M.Y. Song, Rate enhancement of hydrogen generation through the reaction of magnesium hydride with water by MgO addition and ball milling, J. Ind. Eng. Chem. 18 (2012) 405–408. https://doi.org/10.1016/j.jiec.2011.11.104.
[78] S.D. Vincent, J. Huot, Effect of air contamination on ball milling and cold rolling of magnesium hydride, J. Alloys Compd. 509 (2011) L175–L179. https://doi.org/10.1016/j.jallcom.2011.02.147.
[79] H.G. Schimmel, M.R. Johnson, G.J. Kearley, A.J. Ramirez-Cuesta, J. Huot, F.M. Mulder, Structural information on ball milled magnesium hydride from vibrational spectroscopy and ab-initio calculations, J. Alloys Compd. 393 (2005) 1–4. https://doi.org/10.1016/j.jallcom.2004.08.102.
[80] S. Dal Toè, S. Lo Russo, A. Maddalena, G. Principi, A. Saber, et al., Hydrogen desorption from magnesium hydride–graphite nanocomposites produced by ball milling, Mater. Sci. Eng: B. 108 (2004) 24–27. https://doi.org/10.1016/j.mseb.2003.10.030.
[81] J. Charbonnier, P. de Rango, D. Fruchart, S. Miraglia, L. Pontonnier, et al., Hydrogenation of transition element additives (Ti, V) during ball milling of magnesium hydride, J. Alloys Compd. 383 (2004) 205–208. https://doi.org/10.1016/j.jallcom.2004.04.059.
[82] W. Cao, Synthesis of nanomaterials by high energy ball milling, Skyspring Nanomaterials, Inc. (2007).
[83] H. Fecht, E. Hellstern, Z. Fu, W. Johnson, Nanocrystalline metals prepared by high-energy ball milling, Metall. Trans. A. 21 (1990) 2333–2337. https://doi.org/10.1007/BF02646980.
[84] R. Denys, A. Riabov, J. Maehlen, M. Lototsky, J. Solberg, V. Yartys, In situ synchrotron X-ray diffraction studies of hydrogen desorption and absorption properties of Mg and Mg–Mm–Ni after reactive ball milling in hydrogen, Acta Mater. 57 (2009) 3989–4000. https://doi.org/10.1016/j.actamat.2009.05.004.
[85] J. Huot, G. Liang, S. Boily, A. Van Neste, R. Schulz, Structural study and hydrogen sorption kinetics of ball-milled magnesium hydride, J. Alloys Compd. 293 (1999) 495–500. https://doi.org/10.1016/S0925-8388(99)00474-0.
[86] W.S. Tang, J.-N. Chotard, P. Raybaud, R. Janot, Enthalpy–Entropy Compensation Effect in Hydrogen Storage Materials: Striking Example of Alkali Silanides MSiH3 (M = K, Rb, Cs), J. Phys. Chem. C. 118 (2014) 3409–3419. https://doi.org/10.1021/jp411314w.
[87] W. Liu, K.-F. Aguey-Zinsou, Size effects and hydrogen storage properties of Mg nanoparticles synthesised by an electroless reduction method, J. Mater. Chem. A. 2 (2014) 9718–9726. https://doi.org/10.1039/c4ta01108b.
[88] N. Hanada, T. Ichikawa, S.-I. Orimo, H. Fujii, Correlation between hydrogen storage properties and structural characteristics in mechanically milled magnesium hydride MgH2, J. Alloys Compd. 366 (2004) 269–273. https://doi.org/10.1016/s0925-8388(03)00734-5.
[89] R.B.V. Campos, S.A.d.S. Camargo Junior, M.C. Brum, D.S.d. Santos, Hydrogen Uptake Enhancement by the Use of a Magnesium Hydride and Carbon Nanotubes Mixture, Mater. Res. 20 (2017) 85–88. https://doi.org/10.1590/1980-5373-mr-2017-0445.
[90] D.M. Mattox, Handbook of physical vapor deposition (PVD) processing, William Andrew. (2010). https://doi.org/10.1016/C2009-0-18800-1.
[91] Y. Xu, Y. Zhou, Y. Li, Y. Hao, P. Wu, Z. Ding, Recent advances in the preparation methods of magnesium-based hydrogen storage materials, Molecules. 29 (2024) 2451. https://doi.org/10.3390/molecules29112451.
[92] Y. Xu, Y. Li, Q. Hou, Y. Hao, Z. Ding, Ball milling innovations advance Mg-based hydrogen storage materials towards practical applications, Materials. 17 (2024) 2510. https://doi.org/10.3390/ma17112510.
[93] A. Soltani, F. Djani, D.E. Mazouzi, R.N.E. Tiri, A. Aygün, et al., ZnSnO3-SnO2 nanocomposite as a catalyst for efficient hydrogen production through sodium borohydride methanolysis, Int. J. Hydrog. Energy. 67 (2024) 429–437. https://doi.org/10.1016/j.ijhydene.2024.04.208.
[94] M. Song, L. Zhang, F. Wu, H. Zhang, H. Zhao, et al., Recent advances of magnesium hydride as an energy storage material, J. Mater. Sci. Technol. 149 (2023) 99–111. https://doi.org/10.1016/j.jmst.2022.11.032.
[95] D.A. Lanbaran, P.F. Kojour, C. Wang, C. Wen, Z. Wu, et al., Numerical investigation of pulsed heating effects on MgH2 desorption kinetics and thermal efficiency in solid-state hydrogen storage, Appl. Energy. 401 (2025) 126690. https://doi.org/10.1016/j.apenergy.2025.126690.
[96] J.C. Crivello, R.V. Denys, M. Dornheim, M. Felderhoff, D.M. Grant, et al., Mg-based compounds for hydrogen and energy storage, Appl. Phys. A. 122 (2016) 1–17. https://doi.org/10.1007/s00339-016-9601-1.
[97] U. Haussermann, H. Blomqvist, D. Noreus, Bonding and stability of the hydrogen storage material Mg(2)NiH(4), Inorg. Chem. 41 (2002) 3684–3692. https://doi.org/10.1021/ic0201046.
[98] P. Vajeeston, P. Ravindran, M. Fichtner, H. Fjellvag, Influence of crystal structure of bulk phase on the stability of nanoscale phases: investigation on MgH2 derived nanostructures, J. Phys. Chem. C. 116 (2012) 18965–18972. https://doi.org/10.1021/jp305933g.
[99] V. Berube, G. Radtke, M. Dresselhaus, G. Chen, Size effects on the hydrogen storage properties of nanostructured metal hydrides: A review, Int. J. Energy Res. 31 (2007) 637–663. https://doi.org/10.1002/er.1284.
[100] L. Berlouis, P. Honnor, P. Hall, S. Morris, S. Dodd, An investigation of the effect of Ti, Pd and Zr on the dehydriding kinetics of MgH2, J. Mater. Sci. 41 (2006) 6403–6408. https://doi.org/10.1007/s10853-006-0732-1.
[101] A. Kadri, Y. Jia, Z. Chen, X. Yao, Catalytically Enhanced Hydrogen Sorption in Mg-MgH2 by Coupling Vanadium-Based Catalyst and Carbon Nanotubes, Materials. 8 (2015) 3491–3507. https://doi.org/10.3390/ma8063491.
[102] J. Gulicovski, Ž. Rašković-Lovre, S. Kurko, R. Vujasin, Z. Jovanović, et al., Influence of vacant CeO2 nanostructured ceramics on MgH2 hydrogen desorption properties, Ceram. Int. 38 (2012) 1181–1186. https://doi.org/10.1016/j.ceramint.2011.08.047.
[103] S.D. Beattie, U. Setthanan, G.S. McGrady, Thermal desorption of hydrogen from magnesium hydride (MgH2): An in situ microscopy study by environmental SEM and TEM, Int. J. Hydrog. Energy. 36 (2011) 6014–6021. https://doi.org/10.1016/j.ijhydene.2011.02.026.
[104] Y.-h. Zhang, Z.-c. Liu, B.-w. Li, Z.-h. Ma, S.-h. Guo, X.-l. Wang, Structure and electrochemical performances of Mg2Ni1−xMnx (x= 0–0.4) electrode alloys prepared by melt spinning, Electrochim. Acta. 56 (2010) 427–434. https://doi.org/10.1016/j.electacta.2010.08.058.
[105] Y.S. Au, M. Ponthieu, R. van Zwienen, C. Zlotea, F. Cuevas, et al., Synthesis of Mg 2 Cu nanoparticles on carbon supports with enhanced hydrogen sorption kinetics, J. Mater. Chem. A. 1 (2013) 9983–9991. https://doi.org/10.1039/C3TA10926G.
[106] M. Danaie, D. Mitlin, TEM analysis and sorption properties of high-energy milled MgH2 powders, J. Alloys Compd. 476 (2009) 590–598. https://doi.org/10.1016/j.jallcom.2008.09.078.

[107] C. Shang, Z. Guo, Effect of carbon on hydrogen desorption and absorption of mechanically milled MgH2, J. Power Sources. 129 (2004) 73–80. https://doi.org/10.1016/j.jpowsour.2003.11.013.
[108] N. Hanada, T. Ichikawa, H. Fujii, Catalytic effect of Ni nano-particle and Nb oxide on H-desorption properties in MgH2 prepared by ball milling, J. Alloys Compd. 404 (2005) 716–719. https://doi.org/10.1016/j.jallcom.2004.12.166.
[109] H. Simchi, A. Kaflou, A. Simchi, Synergetic effect of Ni and Nb2O5 on dehydrogenation properties of nanostructured MgH2 synthesized by high-energy mechanical alloying, Int. J. Hydrog. Energy. 34 (2009) 7724–7730. https://doi.org/10.1016/j.ijhydene.2009.07.038.
[110] V. Fuster, G. Urretavizcaya, F. Castro, Characterization of MgH2 formation by low-energy ball-milling of Mg and Mg+ C (graphite) mixtures under H2 atmosphere, J. Alloys Compd. 481 (2009) 673–680. https://doi.org/10.1016/j.jallcom.2009.03.056.
[111] P.-A. Huhn, M. Dornheim, T. Klassen, R. Bormann, Thermal stability of nanocrystalline magnesium for hydrogen storage, J. Alloys Compd. 404 (2005) 499–502. https://doi.org/10.1016/j.jallcom.2004.10.087.
[112] O. Friedrichs, F. Aguey-Zinsou, J.A. Fernandez, J. Sanchez-Lopez, A. Justo, et al., MgH2 with Nb2O5 as additive, for hydrogen storage: Chemical, structural and kinetic behavior with heating, Acta Mater. 54 (2006) 105–110. https://doi.org/10.1016/j.actamat.2005.08.024.
[113] M. Polanski, J. Bystrzycki, Comparative studies of the influence of different nano-sized metal oxides on the hydrogen sorption properties of magnesium hydride, J. Alloys Compd. 486 (2009) 697–701. https://doi.org/10.1016/j.jallcom.2009.07.042.
[114] M. Verón, H. Troiani, F. Gennari, Synergetic effect of Co and carbon nanotubes on MgH2 sorption properties, Carbon. 49 (2011) 2413–2423. https://doi.org/10.1016/j.carbon.2011.02.008.
[115] A. Ranjbar, Z. Guo, X. Yu, D. Attard, A. Calka, H.-K. Liu, Effects of SiC nanoparticles with and without Ni on the hydrogen storage properties of MgH2, Int. J. Hydrog. Energy. 34 (2009) 7263–7268. https://doi.org/10.1016/j.ijhydene.2009.07.005.
[116] S.-A. Jin, J.-H. Shim, Y.W. Cho, K.-W. Yi, Dehydrogenation and hydrogenation characteristics of MgH2 with transition metal fluorides, J. Power Sources. 172 (2007) 859–862. https://doi.org/10.1016/j.jpowsour.2007.04.090.
[117] T. Czujko, Z. Zaranski, I. Malka, Z. Wronski, Composite behaviour of MgH2 and complex hydride mixtures synthesized by ball milling, J. Alloys Compd. 509 (2011) S604–S607. https://doi.org/10.1016/j.jallcom.2010.08.133.
[118] C. Wu, P. Wang, X. Yao, C. Liu, D. Chen, G. Lu, H. Cheng, Effect of carbon/noncarbon addition on hydrogen storage behaviors of magnesium hydride, J. Alloys Compd. 414 (2006) 259–264. https://doi.org/10.1016/j.jallcom.2005.07.021.
[119] H. Gasan, O.N. Celik, N. Aydinbeyli, Y.M. Yaman, Effect of V, Nb, Ti and graphite additions on the hydrogen desorption temperature of magnesium hydride, Int. J. Hydrog. Energy. 37 (2012) 1912–1918. https://doi.org/10.1016/j.ijhydene.2011.05.086.
[120] C.J. Webb, A review of catalyst-enhanced magnesium hydride as a hydrogen storage material, J. Phys. Chem. Solids. 84 (2015) 96–106. https://doi.org/10.1016/j.jpcs.2014.06.014.
[121] R. Gremaud, C.P. Broedersz, D.M. Borsa, A. Borgschulte, P. Mauron, et al., Hydrogenography: an optical combinatorial method to find new light-weight hydrogen-storage materials, Adv. Mater. 19 (2007) 2813–2817. https://doi.org/10.1002/adma.200602560.
[122] G. Cao, Nanostructures & nanomaterials: synthesis, properties & applications, Imperial College Press. (2004). https://doi.org/10.1021/ja0409457.
[123] L. Garcia, C. Dinoi, M.F. Mahon, L. Maron, M.S. Hill, Magnesium hydride alkene insertion and catalytic hydrosilylation, Chem. Sci. 10 (2019) 8108–8118. https://doi.org/10.1039/c9sc02056j.
[124] M. Martin, C. Gommel, C. Borkhart, E. Fromm, Absorption and desorption kinetics of hydrogen storage alloys, J. Alloys Compd. 238 (1996) 193–201. https://doi.org/10.1016/0925-8388(96)02217-7.
[125] A. Khawam, D.R. Flanagan, Solid-state kinetic models: basics and mathematical fundamentals, J. Phys. Chem. B. 110 (2006) 17315–17328. https://doi.org/10.1021/jp062746a.
[126] M. Pozzo, D. Alfe, Hydrogen dissociation and diffusion on transition metal (= Ti, Zr, V, Fe, Ru, Co, Rh, Ni, Pd, Cu, Ag)-doped Mg (0001) surfaces, Int. J. Hydrog. Energy. 34 (2009) 1922–1930. https://doi.org/10.1016/j.ijhydene.2008.11.109.
[127] M. Pozzo, D. Alfe, A. Amieiro, S. French, A. Pratt, Hydrogen dissociation and diffusion on Ni- and Ti-doped Mg(0001) surfaces, J. Chem. Phys. 128 (2008) 094703. https://doi.org/10.1063/1.2835541.
[128] P. Spatz, H. Aebischer, A. Krozer, L. Schlapbach, The diffusion of H in Mg and the nucleation and growth of MgH2 in thin films, Z. Phys. Chem. 181 (1993) 393–397. https://doi.org/10.1524/zpch.1993.181.Part_1_2.393.
[129] M. Zhu, Y. Lu, L. Ouyang, H. Wang, Thermodynamic Tuning of Mg-Based Hydrogen Storage Alloys: A Review, Materials (Basel). 6 (2013) 4654–4674. https://doi.org/10.3390/ma6104654.
[130] H. Wang, H.J. Lin, W.T. Cai, L.Z. Ouyang, M. Zhu, Tuning kinetics and thermodynamics of hydrogen storage in light metal element based systems – A review of recent progress, J. Alloys Compd. 658 (2016) 280–300. https://doi.org/10.1016/j.jallcom.2015.10.090.
[131] H. Lin, L. Ouyang, H. Wang, D. Zhao, W. Wang, et al., Hydrogen storage properties of Mg–Ce–Ni nanocomposite induced from amorphous precursor with the highest Mg content, Int. J. Hydrog. Energy. 37 (2012) 14329–14335. https://doi.org/10.1016/j.ijhydene.2012.07.073.
[132] L. Ouyang, F. Qin, M. Zhu, The hydrogen storage behavior of Mg3La and Mg3LaNi0.1, Scr. Mater. 55 (2006) 1075–1078. https://doi.org/10.1016/j.scriptamat.2006.08.052.
[133] V. Skripnyuk, E. Rabkin, Mg3Cd: A model alloy for studying the destabilization of magnesium hydride, Int. J. Hydrog. Energy. 37 (2012) 10724–10732. https://doi.org/10.1016/j.ijhydene.2012.04.065.
[134] T.Z. Si, J.B. Zhang, D.M. Liu, Q.A. Zhang, A new reversible Mg3Ag–H2 system for hydrogen storage, J. Alloys Compd. 581 (2013) 246–249. https://doi.org/10.1016/j.jallcom.2013.07.054.
[135] A. Asselli, J. Huot, Investigation of Effect of Milling Atmosphere and Starting Composition on Mg2FeH6 Formation, Metals. 4 (2014) 388–400. https://doi.org/10.3390/met4030388.
[136] X. Xiao, C. Xu, J. Shao, L. Zhang, T. Qin, et al., Remarkable hydrogen desorption properties and mechanisms of the Mg2FeH6@MgH2core–shell nanostructure, J. Mater. Chem. A. 3 (2015) 5517–5524. https://doi.org/10.1039/c4ta06837h.
[137] S. Garrier, B. Delhomme, P. De Rango, P. Marty, D. Fruchart, S. Miraglia, A new MgH2 tank concept using a phase-change material to store the heat of reaction, Int. J. Hydrog. Energy. 38 (2013) 9766–9771. https://doi.org/10.1016/j.ijhydene.2013.05.026.
[138] S. Vincent, J. Lang, J. Huot, Addition of catalysts to magnesium hydride by means of cold rolling, J. Alloys Compd. 512 (2012) 290–295. https://doi.org/10.1016/j.jallcom.2011.09.084.
[139] L.-P. Ma, P. Wang, X.-D. Kang, H.-M. Cheng, Preliminary investigation on the catalytic mechanism of TiF3 additive in MgH2–TiF3H-storage system, J. Mater. Res. 22 (2007) 1779–1786. https://doi.org/10.1557/jmr.2007.0239.
[140] C. Zhou, Z.Z. Fang, C. Ren, J. Li, J. Lu, Effect of Ti Intermetallic Catalysts on Hydrogen Storage Properties of Magnesium Hydride, J. Phys. Chem. C. 117 (2013) 12973–12980. https://doi.org/10.1021/jp402770p.
[141] C. Lu, J. Zou, X. Shi, X. Zeng, W. Ding, Synthesis and hydrogen storage properties of core–shell structured binary Mg@Ti and ternary Mg@Ti@Ni composites, Int. J. Hydrog. Energy. 42 (2017) 2239–2247. https://doi.org/10.1016/j.ijhydene.2016.10.088.
[142] D. Croston, D. Grant, G. Walker, The catalytic effect of titanium oxide based additives on the dehydrogenation and

hydrogenation of milled MgH2, J. Alloys Compd. 492 (2010) 251–258. https://doi.org/10.1016/j.jallcom.2009.10.199.
[143] J. Cui, H. Wang, J. Liu, L. Ouyang, Q. Zhang, et al., Remarkable enhancement in dehydrogenation of MgH2 by a nano-coating of multi-valence Ti-based catalysts, J. Mater. Chem. A. 1 (2013) 5603–5611. https://doi.org/10.1039/C3TA01332D.
[144] J. Lu, Y.J. Choi, Z.Z. Fang, H.Y. Sohn, E. Ronnebro, Hydrogenation of nanocrystalline Mg at room temperature in the presence of TiH2, J. Am. Chem. Soc. 132 (2010) 6616–6617. https://doi.org/10.1021/ja910944w.
[145] W. Oelerich, T. Klassen, R. Bormann, Mg-based hydrogen storage materials with improved hydrogen sorption, Mater. Transact. 42 (2001) 1588–1592. https://doi.org/10.2320/matertrans.42.1588.
[146] P. Wang, A. Wang, H. Zhang, B. Ding, Z. Hu, Hydrogenation characteristics of Mg–TiO2 (rutile) composite, J. Alloys Compd. 313 (2000) 218–223. https://doi.org/10.1016/S0925-8388(00)01188-9.
[147] W. Kalisvaart, C. Harrower, J. Haagsma, B. Zahiri, E. Luber, et al., Hydrogen storage in binary and ternary Mg-based alloys: A comprehensive experimental study, Int. J. Hydrog. Energy. 35 (2010) 2091–2103. https://doi.org/10.1016/j.ijhydene.2009.12.013.
[148] X. Yao, C. Wu, A. Du, J. Zou, Z. Zhu, et al., Metallic and carbon nanotube-catalyzed coupling of hydrogenation in magnesium, J. Am. Chem. Soc. 129 (2007) 15650–15654. https://doi.org/10.1021/ja0751431.
[149] B. Vigeholm, J. Kjøller, B. Larsen, A.S. Pedersen, Formation and decomposition of magnesium hydride, J. Less-Common Met. 89 (1983) 135–144. https://doi.org/10.1016/0022-5088(83)90259-X.
[150] A. Kucharczyk, K. Naplocha, J.W. Kaczmar, H. Dieringa, K.U. Kainer, Current Status and Recent Developments in Porous Magnesium Fabrication, Adv. Eng. Mater. 20 (2017) 1700562. https://doi.org/10.1002/adem.201700562.
[151] D.-H. Yang, B.-Y. Hur, S.-R. Yang, Study on fabrication and foaming mechanism of Mg foam using CaCO3 as blowing agent, J. Alloys Compd. 461 (2008) 221–227. https://doi.org/10.1016/j.jallcom.2007.07.098.
[152] P. Li, N.V. Nguyen, H. Hao, Dynamic compressive behaviour of Mg foams manufactured by the direct foaming process, Mater. Design. 89 (2016) 636–641. https://doi.org/10.1016/j.matdes.2015.10.021.
[153] N.T. Kirkland, I. Kolbeinsson, T. Woodfield, G. Dias, M.P. Staiger, Processing-property relationships of as-cast magnesium foams with controllable architecture, Int. J. Mod. Phys. B. 23 (2009) 1002–1008. https://doi.org/10.1142/S0217979209060373.
[154] A. Jinnapat, A. Kennedy, The manufacture of spherical salt beads and their use as dissolvable templates for the production of cellular solids via a powder metallurgy route, J. Alloys Compd. 499 (2010) 43–47. https://doi.org/10.1016/j.jallcom.2010.03.132.
[155] F. Witte, H. Ulrich, M. Rudert, E. Willbold, Biodegradable magnesium scaffolds: Part 1: appropriate inflammatory response, J. Biomed. Mater. Res. A. 81 (2007) 748–756. https://doi.org/10.1002/jbm.a.31170.
[156] J. Capek, D. Vojtech, Properties of porous magnesium prepared by powder metallurgy, Mater. Sci. Eng. C. Mater. Biol. Appl. 33 (2013) 564–569. https://doi.org/10.1016/j.msec.2012.10.002.
[157] Z.-k. Xie, M. Tane, S.-k. Hyun, Y. Okuda, H. Nakajima, Vibration–damping capacity of lotus-type porous magnesium, Mater. Sci. Eng: A. 417 (2006) 129–133. https://doi.org/10.1016/j.msea.2005.10.061.
[158] A.H. Yusop, A.A. Bakir, N.A. Shaharom, M.R. Abdul Kadir, H. Hermawan, Porous biodegradable metals for hard tissue scaffolds: a review, Int. J. Biomater. 2012 (2012) 641430. https://doi.org/10.1155/2012/641430.
[159] Y. Bi, Y. Zheng, Y. Li, Microstructure and mechanical properties of sintered porous magnesium using polymethyl methacrylate as the space holder, Mater. Lett. 161 (2015) 583–586. https://doi.org/10.1016/j.matlet.2015.09.039.
[160] X. Wang, Z. Li, Y. Huang, K. Wang, X. Wang, F. Han, Processing of magnesium foams by weakly corrosive and highly flexible space holder materials, Mater. Design. 64 (2014) 324–329. https://doi.org/10.1016/j.matdes.2014.07.049.
[161] C. Zhou, Z.Z. Fang, J. Lu, X. Zhang, Thermodynamic and kinetic destabilization of magnesium hydride using Mg-In solid solution alloys, J. Am. Chem. Soc. 135 (2013) 10982–10985. https://doi.org/10.1021/ja4058794.
[162] S. Agarwal, A. Aurora, A. Jain, I. Jain, A. Montone, Catalytic effect of ZrCrNi alloy on hydriding properties of MgH2, Int. J. Hydrog. Energy. 34 (2009) 9157–9162. https://doi.org/10.1016/j.ijhydene.2009.09.034.
[163] S. Brutti, G. Mulas, E. Piciollo, S. Panero, P. Reale, Magnesium hydride as a high capacity negative electrode for lithium ion batteries, J. Mater. Chem. 22 (2012) 14531–14537. https://doi.org/10.1039/c2jm31827j.
[164] A. Chaise, P. de Rango, P. Marty, D. Fruchart, Experimental and numerical study of a magnesium hydride tank, Int. J. Hydrog. Energy. 35 (2010) 6311–6322. https://doi.org/10.1016/j.ijhydene.2010.03.057.
[165] V. Berube, M. Dresselhaus, G. Chen, Entropy stabilization of deformed regions characterized by an excess volume for hydrogen storage applications, Int. J. Hydrog. Energy. 34 (2009) 1862–1872. https://doi.org/10.1016/j.ijhydene.2008.11.096.